Published in final edited form as:
Toxicol Appl Pharmacol. 2011 October 15; 256(2): 154–167. doi:10.1016/j.taap.2011.08.002.

Non-additive hepatic gene expression elicited by 2,3,7,8-tetrachlorodibenzo-*p*-dioxin (TCDD) and 2,2′,4,4′,5,5′-hexachlorobiphenyl (PCB153) co-treatment in C57BL/6 mice

Anna K. Kopec[a,b], **Michelle L. D. Souza**[a,b], **Bryan D. Mets**[a], **Lyle D. Burgoon**[a,b,c], **Sarah E. Reese**[e], **Kellie J. Archer**[e], **Dave Potter**[f], **Colleen Tashiro**[f], **Bonnie Sharratt**[f], **Jack R. Harkema**[b,d], and **Timothy R. Zacharewski**[a,b,*]

[a]Department of Biochemistry & Molecular Biology, Michigan State University, East Lansing MI, 48824

[b]Center for Integrative Toxicology, Michigan State University, East Lansing MI, 48824

[c]Gene Expression in Development and Disease Initiative, Michigan State University, East Lansing MI, 48824

[d]Pathobiology and Diagnostic Investigations, Michigan State University, East Lansing MI, 48824

[e]Department of Biostatistics, Virginia Commonwealth University, Richmond VA, 23298-0032

[f]Wellington Laboratories Inc., Guelph ON, N1G 3M5, Canada

Abstract

Interactions between environmental contaminants can lead to non-additive effects that may affect the toxicity and risk assessment of a mixture. Comprehensive time course and dose-response studies with 2,3,7,8-tetrachlorodibenzo-*p*-dioxin (TCDD), non-dioxin-like 2,2′,4,4′,5,5′-hexachlorobiphenyl (PCB153) and their mixture were performed in immature, ovariectomized C57BL/6 mice. Mice were gavaged once with 30 μg/kg TCDD, 300 mg/kg PCB153, a mixture of 30 μg/kg TCDD with 300 mg/kg PCB153 (MIX) or sesame oil vehicle for 4,12, 24,72 or 168 h. In the 24 h dose-response study, animals were gavaged with TCDD (0.3,1, 3, 6, 10, 15, 30, 45 μg/kg), PCB153 (3,10, 30, 60, 100, 150, 300, 450 mg/kg), MIX (0.3+3, 1+10, 3+30, 6+60, 10+100, 15+150, 30+300, 45 μg/kg TCDD+450 mg/kg PCB153, respectively) or vehicle. All three treatments significantly increased relative liver weights (RLW), with MIX eliciting significantly greater increases compared to TCDD and PCB153 alone. Histologically, MIX induced hepatocellular hypertrophy, vacuolization, inflammation, hyperplasia and necrosis, a combination of TCDD and PCB153 responses. Complementary lipid analyses identified significant increases in hepatic triglycerides in MIX and TCDD samples, while PCB153 had no effect on lipids. Hepatic

*Corresponding author: Timothy R. Zacharewski, Ph.D., Department of Biochemistry & Molecular Biology, Center for Integrative Toxicology, 501 Biochemistry Building, Wilson Road, Michigan State University, East Lansing, MI 48824-1319, Fax: 517-353-9334, tzachare@msu.edu.

PCB153 levels were also significantly increased with TCDD co-treatment. Microarray analysis identified 167 TCDD, 185 PCB153 and 388 MIX unique differentially expressed genes. Statistical modeling of quantitative real-time PCR analysis of Pla2g12a, Serpinb6a, Nqo1, Srxn1, and Dysf verified non-additive expression following MIX treatment compared to TCDD and PCB153 alone. In summary, TCDD and PCB153 co-treatment elicited specific non-additive gene expression effects that are consistent with RLW increases, histopathology, and hepatic lipid accumulation.

Keywords

TCDD; PCB153; dose-response; mixture; non-additive interaction; liver; gene expression

INTRODUCTION

Polyhalogenated aromatic hydrocarbons (PHAHs), including polychlorinated biphenyls (PCBs) and polychlorinated dibenzo-*p*-dioxins (PCDDs) are persistent environmental contaminants that elicit species- and tissue-specific toxic effects. 2,3,7,8-Tetrachlorodibenzo-*p*-dioxin (TCDD) and other PCDDs are by-products of various activities including municipal solid waste and sewage sludge incineration, herbicide production, pulp and paper bleaching, backyard barrel burning, and other processes (Poland and Glover 1973; Safe et al. 1982; Mason and Safe 1986; Commoner et al. 1987). Despite banning the production and use of PCBs in many industrial applications in the late 1970s (Safe et al. 1982; Mullin et al. 1984; Safe 1990), they are still present in the environment and pose a potential health concern. The chemical stability of PCBs and PCDDs coupled with their lipophilic nature has led to bioaccumulation and biomagnification in the food chain, particularly in fatty tissues (Kimbrough 1995; Safe 1997).

The broad spectrum of effects elicited by PCBs and PCDDs include hepatotoxicity, immune suppression, reproductive toxicity, endocrine disruption, developmental toxicity, and carcinogenicity (Poland and Knutson 1982; Knerr and Schrenk 2006). Overall toxicity is determined by the chemical s structural similarity to TCDD, and ability to bind and activate the aryl hydrocarbon receptor (AhR) (Van den Berg et al. 2006). PCB congeners containing *meta* and *para* chlorines on the biphenyl ring assume coplanar conformation, resembling dioxin (dioxin-like PCBs), and are more toxic than non-coplanar PCBs possessing *ortho* chlorine substituents which have reduced AhR binding affinity (Safe 1990; Safe 1994).

The effects of dioxin and dioxin-like PCBs are mediated through the activation of AhR, a cytosolic basic helix-loop-helix periodicity-AhR nuclear translocator (ARNT)-simple-minded domain containing transcription factor (Poland and Knutson 1982; Denison and Heath-Pagliuso 1998; Safe 2001; Denison et al. 2002). Following ligand binding, chaperone proteins dissociate from the AhR, allowing translocation to the nucleus and heterodimerization with ARNT. AhR:ARNT heterodimers interact with dioxin response elements (DREs) in the regulatory regions of target genes, leading to changes in gene expression (Denison and Heath-Pagliuso 1998; Nebert et al. 2000).

The non-dioxin-like, non-coplanar 2,2′,4,4′,5,5′-hexachlorobiphenyl (PCB153) is the PCB congener at the highest concentrations in human tissue on molar basis, and is found in high

concentrations in environmental and other biological samples (Schecter et al. 1994; NTP 2006a). PCB153 does not bind or activate the AhR, but elicits constitutive androstane receptor (CAR)/pregnane X receptor (PXR)-mediated responses (Craft et al. 2002; Honkakoski et al. 2003; Tabb et al. 2004; Kopec et al. 2010b). Following ligand activation, CAR/PXR translocates to the nucleus to heterodimerize with the retinoid X receptor and binds to CAR and PXR response elements (CAREs and PXREs) in the regulatory regions of target genes to elicit changes in gene expression (Blumberg and Evans 1998; Masahiko and Honkakoski 2000; Lemaire et al. 2007).

Traditionally, environmental risk assessments have focused on single congener exposures. However, PCBs and dioxins exist as complex mixtures, and their interactions can influence the toxicity of a mixture. For example, interactions could include additive effects, or non-additive responses (i.e., synergistic or antagonistic) (Staal et al. 2007). Previous studies have reported non-additive interactions between PCB153 and dioxin-like chemicals including the inhibition of TCDD- and PCB126-induced cleft palate and immunotoxicity, and suppression of ethoxyresorufin-O-deethylase (EROD) (Biegel et al. 1989; Zhao et al. 1997; Suh et al. 2003). In contrast, others reported synergistic induction in mouse hepatic EROD and aryl hydrocarbon hydroxylase activities compared to TCDD treatment alone (Bannister and Safe 1987). Co-treatment has also been shown to elicit synergistic effects on porphyrin accumulation in Sprague-Dawley rats (van Birgelen et al. 1996a). However, no study has examined the non-additive effects of PCB153 and TCDD co-treatment on gene expression.

In this report, time course and dose-dependent hepatic gene expression studies with complementary computational response element searches, histopathology, lipid profiling and tissue analyses of PCB153 and TCDD levels were performed to evaluate the hepatic effects elicited by a mixture of TCDD and PCB153 in immature, ovariectomized C57BL/6 mice. This study complements our previous report (Kopec et al. 2010b) by examining the dose-dependent mixture effects elicited by PCB153 and TCDD. More specifically, dose-response non-linear logistic modeling identified non-additive gene expression interactions that are consistent with the non-additive phenotypic responses elicited by TCDD and PCB153 co-treatment.

MATERIALS AND METHODS

Animal Husbandry

Female C57BL/6 mice, ovariectomized by the supplier on postnatal day (PND) 20, with body weights (BW) within 10% of the average, were obtained from Charles Rivers Laboratories (Portage, MI) on PND 25. Animals were housed in polycarbonate cages containing cellulose fiber chips (Aspen Chip Laboratory Bedding, Northeastern Products, Warrensberg, NY) with 30–40% humidity and a 12 h light/dark cycle (07:00 h – 19:00 h), had free access to deionized water and were fed *ad libitum* with Harlan Teklad 22/5 Rodent Diet 8640 (Madison, WI). Animals were acclimatized prior to dosing on PND 28. Immature ovariectomized mice were used to facilitate comparisons with other data sets obtained using the same model, study design and analysis methods (Boverhof et al. 2005; Kopec et al. 2008; Kopec et al. 2010a). Immature animals are more responsive to AhR ligands, and ovariectomy negates potential interactions with estrogens produced by the maturing ovaries.

All procedures were carried out with the approval of the Michigan State University All-University Committee on Animal Use and Care.

Time Course and Dose-Response Studies

A stock solution of PCB153 (99.9% purity, AccuStandard, New Haven, CT) was first dissolved in acetone (J.T. Baker), followed by dilution with sesame oil (Sigma, St. Louis, MO), and evaporation of acetone under nitrogen gas. A stock solution of TCDD was a gift from the Dow Chemical Company (Midland, MI). PCB153 and TCDD stock solutions were diluted using sesame oil to achieve the desired dose. Animals were orally gavaged using 1.5 inch feeding needles with 2.25 mm ball ends (Cadence Science, Lake Success, NY). For the time course study, mice (n=5 per group) were administered 0.1 ml of a single dose of 30 μg/kg TCDD, 300 mg/kg PCB153, a mixture (MIX) of 1:10,000 ratio of TCDD:PCB153 (30 μg/kg TCDD with 300 mg/kg PCB153) or sesame oil vehicle and sacrificed after 4, 12, 24, 72 or 168 h. Individual TCDD and PCB153 treatments have been published (Kopec et al. 2010b). The time points and doses used were selected to facilitate comparisons with previous studies (Boverhof et al. 2005; Boverhof et al. 2006; Kopec et al. 2008; Kopec et al. 2010a). 30 μg/kg TCDD was selected because it elicited maximum induction of Cyp1a1 mRNA levels without inducing significant changes in body weight gain (Boverhof et al. 2005). 300 mg/kg PCB153 was selected based on a previous dose-response study (Kopec et al. 2010b), eliciting maximum induction of Cyp2b10 mRNA levels and having no negative effect on body weight gain. The mixture (30 μg/kg TCDD+300 mg/kg PCB153) was selected based on the characterized responses of the individual components. The ratio of 1:10,000 TCDD:PCB153 approaches reports of the relative concentrations of TCDD and PCB153 in human samples (Schecter et al. 1994).

In the dose-response study, mice (n=5 per group) were gavaged with TCDD (0.3, 1, 3, 6, 10, 15, 30, 45 μg/kg), PCB153 (3, 10, 30, 60, 100, 150, 300, 450 mg/kg), MIX (0.3+3, 1+10, 3+30, 6+60, 10+100, 15+150, 30+300, 45 μg/kg TCDD + 450 mg/kg PCB153, respectively) or vehicle, and sacrificed 24 h post dose by cervical dislocation. Livers were removed, sections were weighed, flash frozen in liquid nitrogen, and stored at −80°C. A section of the right liver lobe was fixed in 10% neutral buffered formalin (Sigma) for histological analysis. For lipid staining, the remaining right lobe of the liver was frozen in Tissue-Tek O.C.T. compound (Sakura, Torrance, CA).

Histological Analysis

Fixed liver tissues were sectioned and processed in ethanol, xylene, and paraffin using a Thermo Electron Excelsior tissue processor (Waltham, MA). Tissues were embedded in paraffin with Miles Tissue Tek II embedding center, after which paraffin blocks were sectioned at 5 μm with a rotary microtome. Liver sections were placed on glass microscope slides, washed twice in xylene for 5 min, followed by four quick washes in ethanol and rinsing in water. Slides were placed in Gill 2 hematoxylin (Thermo Fisher Scientific, Waltham, MA) for 1.5 min followed by 2–3 quick dips in 1% glacial acetic acid water and rinsed with running water for 2–3 min. Slides were then rinsed in ethanol and counterstained with 1% eosin Y-phloxine B solution (Sigma) followed by multiple rinses in ethanol and xylene.

For lipid staining, liver samples were sectioned at 6 μm, fixed in 10% neutral buffered formalin for 5 min, rinsed with water and immersed in 100% propylene glycol for 5 min. Slides were stained with Oil Red O solution (Sigma) for 8 min at 60°C, placed in 80% propylene glycol for 5 min and rinsed in water for 15 min. Slides were counterstained with Gill 2 hematoxylin for 30 sec and washed with water for 30 min. Coverslips were attached using aqueous mounting media. All the histological processing was performed at Michigan State University Investigative Histopathology Laboratory, Division of Human Pathology using a modified version of previously published procedures (Sheehan and Hrapchak 1980).

Lipid Analysis by Gas Chromatography-Mass Spectrometry (GC-MS)

TCDD, PCB153, MIX and vehicle control liver samples (~100 mg) from the time course (24, 72, 168 h) and dose-response (24 h) studies were homogenized (Polytron PT2100, Kinematica AG, Luzern, CH) in 40% methanol and acidified with concentrated HCl. Lipids were extracted with chloroform:methanol (2:1) containing 1 mM 2,6-di-tert-butyl-4-methylphenol (B HT; Sigma) and extraction efficiency controls (19:1n9 FFA [free fatty acid] and 19:0 TAG [triacylglycerol]) were added (Nu-Chek Prep, Elysian, MN). Protein and aqueous phases were re-extracted with chloroform and the organic phases were pooled. A derivatization standard (19:2n6 FFA; Nu-Chek Prep) was added and samples were dried under nitrogen, resuspended in 2% non-aqueous methanolic HCl and incubated at 60°C overnight. Samples were cooled to room temperature and 0.9% (w/v) NaCl and hexane were added. The organic phase was collected and a loading control (17:1n9 fatty acid methyl ester [FAME]; Nu-Chek Prep) was added. Samples were dried under nitrogen, resuspended in equal volumes of hexane and separated on Agilent 6890N gas chromatograph interfaced to Agilent 5973 mass spectrometer with DB23 column (30 m length, 0.25 mm internal diameter, 0.25 μm film thickness). Samples were run on the following temperature program: 50°C to 150°C at 40°C/min, to 185°C at 5°C/min, to 235°C at 3°C/min, to 250°C at 10°C/min. Peak areas were integrated with MassLynx software (Waters, Milford, MA) and data were normalized to the starting amount of liver and loading controls. Principal component analysis of temporal lipid profiles (represented as the average fold change induction of the 21 identified fatty acids) was performed in R 2.6.0. Data were extracted and used to generate PCA plots in GraphPad Prism 5.0 (La Jolla, CA).

Hepatic Triglyceride Measurement

Frozen liver samples (~100 mg) were homogenized (Polytron PT2100, Kinematica) in 1 ml of 1.15% KCl. Triglycerides were extracted from 200 μl of hepatic homogenate with 800 μl of isopropyl alcohol by vortex-mixing for 10 min. The samples were centrifuged for 5 min at 800 x g at room temperature and supernatant was collected into separate vials. The concentration of hepatic triglycerides was determined using a commercial L-Type Triglyceride M kit (Wako Diagnostics, Richmond, VA) with Multi-Calibrator Lipids as a standard (Wako Diagnostics). The measurements were performed according to the manufacturer's protocol with 20 μl of the triglyceride extract incubated with 150 μl of Reagent 1 followed by incubation with 50 μl of Reagent 2. Final results were normalized to the starting amount of liver (Supplementary Fig. 5).

Quantification of Hepatic PCB153 and TCDD Levels

Liver samples were processed in parallel with laboratory blanks and a reference or background sample at Wellington Laboratories Inc. (Guelph, ON, Canada). Samples (100 to 500 mg) were transferred to a tared screw cap culture tube and weights were recorded. Samples were spiked with $^{13}C_{12}$-PCB153 and $^{13}C_{12}$-2,3,7,8-TCDD surrogates and digested with hydrochloric acid. Each digested sample was then split between two screw cap tubes and 3–4 ml hexane was added to each tube followed by vigorous mixing. Tubes were centrifuged, and the organic layer was removed. Hexane extraction was repeated three times per screw cap tube and the six hexane fractions were combined. The hexane fraction was then split evenly prior to clean-up and one fraction was archived. The other fraction was cleaned-up using a small multi-layer (acid/base/neutral) silica gel column eluted with 20–25 ml of hexane. The eluate was concentrated on a rotary evaporator and then transferred to a conical microvial with pentane and dichloromethane rinses and allowed to dry. Immediately prior to injection on the high-resolution gas chromatograph/high-resolution mass spectrometer (HRGC-HRMS) system $^{13}C_{12}$-PCB111 and $^{13}C_{12}$-1,2,3,4-TCDD injection standards were added to the conical microvial. The identification and quantification of PCB153 and TCDD was performed using an Agilent (Santa Clara, CA, USA) 6890 series HRGC with direct capillary interface to a Waters Autospec Ultima HRMS. Chromatographic separations were carried out on a 60 m DB5 (0.25 mm ID, 0.25 μm film thickness) column in constant flow mode (Helium, 1 ml/min). All injections were 1 μl and a splitless injection was used. The mass spectrometer was operated in EI+ selective ion recording mode at a mass resolving power of 10,000 or greater. The % recovery ranged between 78–111% for $^{13}C_{12}$-PCB153 and between 80–107% for $^{13}C_{12}$-2,3,7,8-TCDD. The detection limits were 5.5 pg/g (ppt) for TCDD and 44.5 pg/g (ppt) for PCB153.

RNA Isolation

Liver samples (~100 mg stored at −80°C) were immediately transferred to 1 ml TRIzol (Invitrogen, Carlsbad, CA) and homogenized using a Mixer Mill 300 tissue homogenizer (Retsch, Germany). Total RNA was isolated according to the manufacturer s protocol with an additional acid phenol:chloroform extraction. Isolated RNA was resuspended in an RNase-free RNA storage solution (Ambion Inc., Austin, TX) that has a low pH and contains sodium citrate to minimize RNA hydrolysis. RNA was quantified (A_{260}), and quality assessed by determining the A_{260}/A_{280} ratio and by visual inspection of 2 μg on a denaturing gel.

Microarray Experimental Design

TCDD, PCB153, MIX and vehicle RNA samples from the time course study were individually hybridized to 4 × 44 K Agilent microarrays (version 1; Agilent Technologies, Inc., Santa Clara, CA). Three biological replicates were performed using one-color labeling (Cy3) for each time point and treatment, according to the manufacturer s protocol (Agilent Manual: G4140-90040 v. 5.7). Microarray slides were scanned at 532 nm (Cy3) on a GenePix 4000B scanner (Molecular Devices, Union City, CA). Images were analyzed for feature and background intensities using GenePix Pro 6.0 (Molecular Devices). All data were managed in TIMS dbZach data management system (Burgoon and Zacharewski 2007).

Microarray Analysis

All microarray data passed our laboratory quality assurance protocol (Burgoon et al. 2005). Microarray data were normalized using a semi-parametric approach (Eckel et al. 2005) and the posterior probabilities were calculated using an empirical Bayes method based on a per gene and dose basis using model-based *t* values (Eckel et al. 2004). Gene expression data were ranked and prioritized using P1(*t*) values >0.999 and |fold change|>1.5 to identify differentially expressed genes. Individual chemical (TCDD and PCB153) temporal microarray datasets have been published (Kopec et al. 2010b). Data obtained from the time course microarray were used as a screen to identify putative non-additive candidates for further verification using QRTPCR in the 24 h dose-response study. Complete temporal microarray datasets (TCDD, PCB153 and MIX) with corresponding statistics comparing TCDD vs. PCB153, TCDD vs. MIX and MIX vs. PCB153 at each time point are available as Supplementary Table 2.

Quantitative Real-Time PCR (QRTPCR)

QRTPCR verification of microarray responses was performed as described previously (Boverhof et al. 2005). Briefly, 1 μg of total RNA was reverse transcribed by SuperScript II (Invitrogen) using an anchored oligo-dT primer as described by the manufacturer. The cDNA (1.0 μl) was used as a template in a 30 μl PCR reaction containing 0.1 μM of forward and reverse gene-specific primers, 3 mM $MgCl_2$, 1 mM dNTPs, 0.025 IU AmpliTaq Gold, and 1 × SYBR Green PCR buffer (Applied Biosystems, Foster City, CA). Supplementary Table 3 provides the names, abbreviations, accession numbers, forward and reverse primer sequences, and amplicon sizes. PCR amplification was conducted on an Applied Biosystems PRISM 7500 Sequence Detection System. cDNAs were quantified using a standard curve approach and the copy number of each sample was standardized to 3 housekeeping genes (Actb, Gapdh, Hprt) to control for the differences in RNA loading, quality, and cDNA synthesis (Vandesompele et al. 2002). For graphing purposes, the relative expression levels were scaled such that the expression level of the time-matched control group was equal to one.

Computational Putative DNA Response Element Identification

Putative dioxin response elements (DREs) (Sun et al. 2004; Dere et al. 2011a), constitutive androstane receptor response elements (CAREs) (Phillips et al. 2009) and pregnane X receptor response elements (PXREs) (Kopec et al. 2010b) were computationally identified using Position Weight Matrices (PWM) specific to each element. Genomic regions (−10,000 bp relative to the transcriptional start site [TSS] together with 5′-untranslated region [UTR]) were obtained from the University of California, Santa Cruz, Genome Browser for mouse (build 37), computationally searched, and each DRE, CARE and PXRE was scored using a specific PWM. The genomic region 10,000 bp upstream of the TSS and the 5′ UTR was examined to include more distal putative response elements which have recently been identified and may regulate gene expression. These regions were also selected to facilitate comparisons to other studies examing similar regions (Boverhof et al. 2006; Kopec et al. 2010b; Dere et al. 2011a; Dere et al. 2011b). Matrix similarity scores (MSS) >0.80 are considered to be putative response elements.

Dose-Response Non-linear Logistic Modeling

Gene-specific non-linear models were fit to investigate the dose-response relationship for Dysf, Pla2g12a, Serpinb6a, Srxn1, Nqo1, Got1, Elovl5, Dexi, Akr1c20, and Srebf1 identified in the microarray study as putative candidates exhibiting non-additive gene expression and further verified using QRTPCR in the 24 h dose-response study. Specifically, for each gene a non-linear logistic model for the mean was used to estimate the dose-response relationship for TCDD and PCB153, according to:

$$\mu_{add}=\frac{\gamma}{1+\exp-\beta_0+\beta_1 x_1+\beta_2 x_2},$$

where β_0 is the unknown intercept parameter, β_i, $i=1,2$, is the unknown slope parameter associated with the ith single chemical, x_i is the dose associated with the ith chemical, γ is the maximum-effect parameter, and μ_{add} is the expected value of the response under the additive model. Simultaneously, the MIX data were fit with a mixture model:

$$\mu_{mix}=\frac{\gamma}{1+\exp-\beta_0+\theta_{mix}t},$$

where t is the total dose associated with MIX data. For a fixed-ratio of TCDD and PCB153 given by (a_1, a_2, such that $a_1 + a_2 =1$), the slope for the mixture under the assumption of additivity is $\theta_{add}= \beta_1 a_1+ \beta_2 a_2$. Based on preliminary analyses, using the quasi-likelihood estimation criterion, the assumption is made that variance is a function of the mean: $\mathrm{Var}(y)= \tau\mu$, where τ is the parameter associated with the functional form of the variance and has to be estimated. The quasi-likelihood criterion has assumptions only concerning the first and second moments, and some regularity conditions related to the regression equation: $E(Y)= \mu(\theta)$ and $\mathrm{Var}(Y)= \tau V(\mu)$. It is of interest to maximize the quasi-likelihood function given by:

$$Q=\frac{1}{\tau}\int_{\mu}^{y}\frac{y-t}{t}dt=\frac{1}{\tau}y\log\mu-\mu.$$

Gene-specific plots of the mean versus the variance for TCDD, PCB153 and MIX confirmed the relationship between the mean and the variance. In the study, the additive dose-response model for the fixed-ratio mixture based on TCDD and PCB153 data alone was compared to the mixture model obtained using MIX data. Therefore, the null hypothesis tested was $\theta_{mix}= \theta_{add}$, where θ_{mix} and θ_{add} are the parameter estimates assuming the mixture and the additive models, respectively. The modeling (PROC NLIN) was performed with SAS 9.2 (SAS Institute, Cary, NC).

Functional Gene Annotation and Statistical Analysis

Annotation and functional categorization of the differentially regulated genes was performed using Database for Annotation, Visualization and Integrated Discovery (DAVID) (Dennis et al. 2003) and Ingenuity Pathway Analysis (Ingenuity Systems, Redwood City, CA). All statistical analyses were performed with SAS 9.2. Unless stated otherwise, all data were

analyzed by analysis of variance (ANOVA) followed by Dunnett's or Tukey's *post hoc* test. Differences between treatment groups were considered significant when $p<0.05$.

RESULTS

Organ and Body Weights

Exposure to dioxins and PCBs elicits temporal and dose-dependent increases in liver weight in rodents (Denison and Heath-Pagliuso 1998; Craft et al. 2002; Boverhof et al. 2006; NTP 2006a; NTP 2006b; Kopec et al. 2010b). In the time course study, significant increases in relative liver weight (RLW) were observed with 300 mg/kg PCB153 (72, 168 h), 30 μg/kg TCDD and MIX (24, 72, 168 h), relative to time-matched vehicle controls (Fig. 1A). TCDD and PCB153 treatment resulted in comparable increases in RLW, while MIX induced significantly greater increases in RLW compared to TCDD and PCB153 alone at 72 and 168 h (Fig. 1A). These results are consistent with reported increases in RLW in C57BL/6 and B6C3F1 mice 3, 7 and 13 days after a single gavage of TCDD and PCB153 mixture (De Jongh et al. 1995; van Birgelen et al. 1996b).

In the 24 h dose-response study, TCDD and MIX elicited comparable increases in RLW in all but the lowest dose groups (Fig. 1B). RLW increases at 15+150 (μg/kg TCDD + mg/kg PCB153, respectively) were also greater compared to 150 mg/kg PCB153 (Fig. 1B). In contrast, PCB153 increased RLW only at 100 and 300 mg/kg.

Minimal (≤ 10%) decreases in body weight gain were observed with PCB153 (300 and 450 mg/kg) and MIX (three highest dose group combinations) at 24 h, but are not indicative of systemic toxicity (FDA 2008). Supplementary Tables 1A–B provide time course and dose-response data for terminal body weight, body weight gain, liver weight and relative liver weights.

Hepatic Tissue Level Quantification

HRGC-HRMS analysis of liver samples at 24 and 168 h indicate that hepatic PCB153 accumulation was potentiated following TCDD co-treatment compared to PCB153 alone (Fig. 2B). No changes were detected in the hepatic TCDD accumulation following PCB153 co-administration (Fig. 2A). In addition, PCB153 levels dramatically decreased at 168 h, compared to more modest reductions in TCDD levels after seven days (Kopec et al. 2010b).

Histopathology

In the time course study, TCDD elicited moderate multifocal inflammation and marked hepatocellular vacuolization localized in periportal regions, extending to midzonal and centrilobular regions at later time points. Instances of vacuolization corresponded with Oil Red O (ORO) staining indicative of neutral lipid accumulation (Fig. 3B,F, Supplementary Fig. 1B,F). These changes are consistent with the reported hepatic effects of TCDD in mice (Boverhof et al. 2005; Boverhof et al. 2006).

PCB153 elicited vacuolization comparable to levels observed in vehicles, as well as mild to moderate centrilobular hypertrophy with cytoplasmic granularity (Fig. 3C,G) (Kopec et al. 2010b). In contrast, PCB153 did not elicit inflammation, while MIX elicited a combination

of TCDD and PCB153 responses. Vacuolization and ORO staining in MIX were the most severe at 24 h, decreasing to TCDD-exposed levels at 168 h. MIX-treated livers also had moderate multifocal inflammation and a temporal increase in cellular hypertrophy that was comparable to time-matched TCDD and PCB153-exposed livers, respectively. Furthermore, MIX elicited minimal necrosis and instances of mitotic figures indicative of hyperplasia between 72 and 168 h (Fig. 3D,H).

Liver microscopic changes were also dose-responsive (Supplementary Fig. 2). TCDD elicited moderate periportal hepatocellular vacuolization and minimal multifocal inflammation (15, 30, 45 μg/kg), while PCB153 elicited mild to moderate centrilobular hypertrophy (300 and 450 mg/kg) and minimal to mild hepatocellular vacuolization. MIX induced moderate to marked periportal hepatocellular vacuolization and centrilobular hypertrophy and minimal mixed cell infiltration (15+15, 30+300, 45 μg/kg TCDD + 450 mg/kg PCB153, respectively).

Lipid Profiling

Total lipids extracted from TCDD, PCB153, MIX and control livers from the time course (24, 72 and 168 h) and dose-response studies were derivatized to fatty acid methyl esters. Twenty one fatty acid species were measured using GC-MS. Principal component (PC) analysis (Supplementary Fig. 3) identified a time- and treatment-dependent separation of fatty acid (FA) profiles (as fold changes) around PC1 and PC2, respectively. Treatment and time-dependent induction in individual fatty acids is represented in Supplementary Fig 4. TCDD induced the most pronounced changes in total FAs (Table 1), consistent with the ORO staining. MIX-elicited increases in total FAs were comparable across time, with significant changes at 24 and 168 h (Table 1).

TCDD significantly induced saturated (SFA), monounsaturated (MUFA) and n3 and n6 polyunsaturated fatty acids (PUFA) in a time-dependent fashion. In contrast, PCB153 did not change total FAs or any specific FA (Table 1), consistent with the lack of ORO staining, and CAR-mediated inhibition of lipogenesis (Zhai et al. 2010). However, MIX elicited differences in SFA, MUFA, and PUFA levels when compared to individual treatments (Table 1). For example, MIX significantly decreased MUFA and total FA levels (168 h), but increased n6 PUFA (24 h) levels compared to TCDD (Table 1). These effects are consistent with the induction of triglyceride levels by MIX (Supplementary Fig. 5) and ORO staining (Supplementary Fig. 1). GC-MS analysis of the dose-response study also revealed higher FA accumulation in MIX-treated livers compared to TCDD groups, although the differences did not achieve statistical significance (Supplementary Fig. 6).

Temporal Microarray Gene Expression

Hepatic gene expression was evaluated using whole-genome 4×44K Agilent oligonucleotide microarrays containing ~21,000 unique annotated genes. Statistical analysis of the time course data identified 568 unique gene expression changes, with 167, 185 and 388 genes differentially regulated in response to TCDD, PCB153, and MIX, respectively (|fold change| >1.5, P1(t)>0.999) at one or more time points. MIX elicited the highest number of differentially expressed genes at each time point. Even with more stringent fold change

criteria (|fold change|>2.0), MIX consistently elicited the highest number of differentially expressed genes (339 unique genes) relative to TCDD (151 unique genes) and PCB153 (121 unique genes).

Comparative analysis identified 68 TCDD-, 111 PCB153-, and 230 MIX-specific responses (|fold change|>1.5, P1(*t*)>0.999). Only 13 genes were differentially expressed by all three treatments (Fig. 4A). When the statistical criteria were relaxed (|fold change|>1.5, P1(*t*)>0.95) (Fig. 4B), the number of overlapping genes increased. A complementary Venn diagram (|fold change|>2.0) is included (Supplementary Fig. 7A–B).

Functional annotation of the 568 differentially regulated genes was associated with xenobiotic metabolism, oxidoreduction/oxidative stress, lipid metabolism, immune response, cell division and differentiation, cell death, and transport. Many of these over-represented functions (Table 2) could be anchored to the changes in RLW, histopathology, and lipid profiles. For example, the differential expression of genes involved in lipid metabolism and transport was consistent with the hepatic fatty accumulation, increased hepatic triglyceride levels, and changes in specific FAs. TCDD and MIX induced significant fatty vacuolization between 24–168 h consistent with Cd36 (~6 fold) and Fabp12 (~54–34 fold) induction, which were not affected by PCB153. Down-regulation of Elovl5 (~2 fold) and up-regulation of Insig2 (~6 fold) by PCB153, in contrast to TCDD, was also consistent the fatty acid profile indicating a lack of lipid accumulation in PCB153-exposed livers.

Histopathology also revealed alterations in cell size (hypertrophy), as well as cell division and cell death (hyperplasia and necrosis) (Fig. 3 and Supplementary Fig. 2). TCDD and MIX induced genes that promote cell death including Bcl2l11 (~2–4 fold), Tnfaip2 (~7 fold), Tnfaip8l1 (~3–4 fold), Traf5 (~2 fold), and Htatip2 (~4 fold), and were not regulated by PCB153, which did not elicit cell death.

Moreover, TCDD induced immune response genes (~2–8 fold; Clec7a, Fcgr1, H2-Eb1, H2-DMa, H2-DMb1, Irf8, Ltb, Mfg28 and Saa1-3), consistent with the marked multifocal inflammation at later time points. In contrast, PCB153 did not alter the expression of these genes, while MIX elicited significant inflammation, reflected by the induction of the same immune related genes as TCDD treatment alone.

Genes involved in xenobiotic metabolism and oxidoreductase activities exhibited the highest induction by all three treatments. This included cytochrome P450s (e.g. Cyp1a1, Cyp1a2, Cyp2b10, Cyp2b13, Cyp2b9, Cyp2c55, Cyp23a25, Cyp39a1) and glutathione S-transferases (e.g. Gsta2, Gstm2, Gstt2, Gstm4), as well as Nqo1, Ugdh, and Aox1. For example, Cyp1a1 was induced ~348 fold by TCDD and MIX. Unlike treatment-specific induction of Cyp1a (TCDD) and Cyp2b/2c/23a/39a (PCB153) families, MIX elicited the differential expression of all cytochrome P450 subfamilies, suggesting the dual activation of AhR and CAR/PXR pathways. Computational analysis identified putative DREs, CAREs and PXREs in the promoter regions (−10,000 bp relative to the TSS together with the 5′ UTR) of differentially regulated genes (Table 2) (Kopec et al. 2010b; Dere et al. 2011a).

QRTPCR Verification of Microarray Responses

In addition to functional categorization of the gene expression responses, the temporal microarray dataset with corresponding statistics (Supplementary Table 2) were used to identify putative non-additive gene expression in MIX treatment compared to TCDD and PCB153 alone. QRTPCR verified the temporal and dose-dependent expression of 13 genes. Cyp1a1, Cyp2b10, and Cyp3a11 differential expression (Fig. 5) was confirmed as positive controls for AhR, CAR and PXR-mediated responses, respectively (Nebert et al. 1990; Maglich et al. 2002; Honkakoski et al. 2003). Although microarray data suggested that Cyp3a11 was not differentially expressed, it was verified by QRTPCR, resulting in amplification of a different region of the 2053 bp long Cyp3a11 gene relative to the microarray. More specifically, the microarray probe maps the 60-mer region between positions 1105 and 1164, while Cyp3a11 primers amplified the 119 bp fragment between 1701 and 1819 bp suggesting that both techniques amplified non-overlapping regions of the Cyp3a11 gene.

TCDD significantly induced Cyp1a1, while PCB153 induced Cyp2b10 and Cyp3a11. The induction of Cyp1a1, Cyp2b10, and Cyp3a11 by MIX was comparable to TCDD and PCB153 alone, and therefore was not considered for non-additive evaluation.

Statistical Verification of Non-Additive Gene Expression

Analysis of gene expression time course data suggested that Nqo1, Dysf, Pla2g12a, Serpinb6a, Srxn1 (Fig. 6) and Elovl5, Srebf1, Dexi, Got1, Akr1c20 (Supplementary Fig. 8) exhibited potential non-additive interactions. The time course and dose-response profiles elicited by TCDD, PCB153, and MIX were verified using QRTPCR and further examined using gene-specific non-linear models to statistically determine synergistic, antagonistic, or additive interactions. Initial analysis confirmed that the variance is proportional to the mean: $\mathrm{Var}(Y) = \tau V(\mu)$. Linear regression provided parameter estimates used as initial values for β_i's and maximum fold expression for each gene was used as the initial value for γ. The final model fit for the expected value for each gene was:

$$\mu = \frac{\gamma}{1+\exp -\beta_0+\beta_1 x_1 I_1+\beta_2 x_2 I_2+\theta_{mix} t I_3},$$

where β_0 is the unknown intercept, β_1 is the unknown slope parameter associated with TCDD doses, β_2 is the unknown parameter associated with PCB153 doses, θ_{mix} is the parameter associated with doses of the mixture TCDD+PCB153, and I_i are indicator functions for the chemical groups, where:

$$I_i = \begin{cases} 1 & \text{if chemical } i \\ 0 & \text{if not chemical } i \end{cases} \quad \text{for } i = 1, 2, 3,$$

where i=1, i=2, and i=3 represents TCDD, PCB153, and MIX, respectively. The intercept parameter α is assumed to be zero. Plots of the residuals against the predicted values were assessed for goodness of fit of the models, and no abnormalities were found.

To determine statistically significant deviation from additivity, the quasi-likelihood ratio test was used to compare the empirical mixture model with the reduced additivity model based on the F-distribution (Gennings et al. 2002):

$$\mu = \frac{\gamma}{1+\exp -\beta_0+\beta_1 x_1 I_1+\beta_2 x_2 I_2+\theta_{add} t I_3},$$

where $\theta_{add} = \beta_1 a_1 + \beta_2 a_2$, where a_1 and a are the 'mix ratios' for TCDD and PCB153 respectively. The 'mix ratios' were obtained by dividing the dose by the total dose. For example, when the TCDD dose is 1 μg/kg, the PCB153 dose is 10000 μg/kg (10 mg/kg), so the 'mix ratios' are $\alpha_1 = \frac{1}{10000+1} = 0.0001$ and $\alpha_2 = \frac{10000}{10000+1} = 0.9999$ such that $\Sigma_i a_i = 1$.

Each graph in Fig. 7 illustrates the overlay between the additive model generated using TCDD and PCB153 data alone and the mixture model fitted using MIX data for each gene. The quasi-likelihood ratio test determined that the mixture model was significantly ($p<0.0001$) different from the additive model for Nqo1, Dysf, Pla2g12a, Serpinb6a and Srxn1, indicating co-administration of TCDD plus PCB153 elicited synergistic differential gene expression.

Srebf1, Akr1c20 and Dexi approached significant non-additive expression (p=0.0619, p=0.0615, p=0.0806, respectively), while Elovl5 (p=0.5164) and Got1 (p=0.9181) was not significantly different from additivity (Supplementary Fig. 9). Supplementary Table 4 contains summary statistics, parameter values for each gene and results of the quasi-likelihood ratio test.

DISCUSSION

Non-additive interactions confound mixture risk assessment. Therefore special considerations are required, including adequate dose-response characterization for each mixture component, applying a "no-interaction" hypothesis to determine synergy or antagonism, testing mixture components across a sufficient range, using appropriate models to statistically determine departure from additivity, and assessing interactions at relevant levels of biological organization to assure meaningful interpretation of the results (Borgert et al. 2001; Borgert 2007).

This study complements our previous report evaluating the temporal effects of single chemical toxicity (Kopec et al. 2010b), by identifying non-additive dose-dependent effects elicited by a mixture of TCDD and PCB153. The non-additive hepatic differential gene expression was phenotypically anchored and compared to effects elicited by individual TCDD and PCB153 treatments. Statistical modeling confirmed non-additive effects in a subset of differentially expressed genes that could be functionally associated with changes in gross physiology, histopathology, and hepatic lipid composition.

Mixtures of dioxin and non-dioxin-like chemicals increase hepatic disposition compared to single chemical administration (De Jongh et al. 1995). In the current study, hepatic PCB153 levels were significantly increased following co-administration with TCDD at 24 and 168 h.

These results are consistent with rat studies that also reported TCDD co-treatment increased PCB153 levels (Van der Kolk et al. 1992). Co-administration of PCB153 with dioxin-like PCB156 also led to significant hepatic retention of PCB153 after 7 and 14 days in C57BL/6J mice (De Jongh et al. 1992). In B6C3F1 mice, TCDD-elicited increases in PCB153 levels were specific to the liver and not observed in other tissues (van Birgelen et al. 1996b). The NTP co-treatment study (PCB153+PCB126) in Sprague-Dawley rats reported that at high mixture dose combinations, the levels of PCB126 were lower compared to hepatic concentrations of the PCB126 group alone, suggesting that PCB153 antagonizes the accumulation of PCB126 in the liver (NTP 2006d; NTP 2006c). In contrast, TCDD levels did not change with PCB153 co-treatment, as previously reported (De Jongh et al. 1995; van Birgelen et al. 1996b).

Hepatic sequestration of TCDD and other dioxin-like PCBs is mediated by binding to Cyp1a2 protein (DeVito et al. 1998). Cyp1a2 null mice exhibit 10-fold lower hepatic TCDD accumulation compared to wild types (Diliberto et al. 1999). PCB153 has a higher affinity for adipose compared to hepatic tissue (van Birgelen et al. 1996b) and unlike TCDD and dioxin-like PCBs it is not sequestered by Cyp1a2 protein. However, TCDD induces fatty accumulation in the liver (Boverhof et al. 2005), increasing hepatic lipophilicity, which may contribute to hepatic PCB153 accumulation following co-administration with TCDD (Van der Kolk et al. 1992; van Birgelen et al. 1996b).

MIX induced xenobiotic metabolism gene expression, comparable to levels elicited by individual treatments. Cytochrome P450 induction was the highest among all functional categories, and included prototypical AhR (Cyp1a1, Cyp1a2) and CAR/PXR (Cyp2b9, Cyp2b10, Cyp2b13, Cyp23a25, Cyp3a11) regulated genes (Nebert et al. 1990; Maglich et al. 2002; Honkakoski et al. 2003). Nqo1, a known AhR- and nuclear factor erythroid 2-related factor 2 (Nrf2)- inducible gene (Yeager et al. 2009), also displayed non-additive induction following MIX treatment, which may serve cytoprotective roles (Ma et al. 2004; Klaassen and Reisman 2010). In addition, MIX synergistically induced Srxn1, sulfiredoxin 1 homolog, an Nrf2-dependent oxidoreductase, which protects lung tissue from smoke-induced oxidative injury (Park et al. 2009; Singh et al. 2009). Synergistic induction of Nqo1 and Srxn1 may provide additional defense from the xenobiotic stress induced by MIX. Enzyme induction also leads to endoplasmic reticulum proliferation increasing hepatocyte size, which may be a factor in increased RLW induced by MIX compared to TCDD and PCB153 alone.

Among oxidoreductase and xenobiotic metabolism genes, aldo-keto reductase (AKR) superfamily members were also differentially expressed including Akr1b7 and Akr1c19 induction and the repression of Akr1c20. AKRs are involved in NAD(P)H-dependent oxidoreductions of a variety of natural and foreign substrates and have been implicated in alleviating toxicity associated with lipid peroxidation (Liu et al. 2009). Expression of Akr1b7 is abolished in CAR and PXR null mice (Liu et al. 2009), consistent with PCB153 and MIX-mediated Akr1b7 induction. Moreover, putative CAREs and PXREs were identified in the upstream regulatory regions. Statistical modeling approached significant ($p=0.0615$) synergistic repression of Akr1c20 following MIX treatment. Akr1c20 expression is liver-specific, but has unknown function (Matsumoto et al. 2006). Based on structural

similarity to 17β-hydroxysteroid dehydrogenase type 5 and comparable enzymatic properties, Akr1c20 may be involved in steroid metabolism and reduction of non-steroidal α-dicarbonyl compounds (Matsumoto et al. 2006).

Integrating histopathology, ORO staining, GC-MS fatty acid and triglyceride analyses suggests that TCDD- and MIX-elicited hepatic lipid accumulation also contribute to increased RLW. The AhR-mediated fatty accumulation (steatosis) can be associated with the differential expression of lipid transport and metabolism genes. TCDD induces the expression of the fatty acid transporter, Cd36 (Lee et al. 2010), which was also induced by MIX. Cd36 facilitates hepatic uptake of free fatty acids and is up-regulated in non-alcoholic fatty liver disease patients (Greco et al. 2008). TCDD and MIX also induced fatty acid binding protein 12 (Fabp12), which also facilitates hepatic uptake of free fatty acids (Tijet et al. 2006). In contrast, PCB153 treatment alone did not alter Cd36 or Fabp12 expression, consistent with lack of hepatic fat accumulation.

Furthermore, PCB153 down-regulated a number of lipid metabolism genes, including Elovl5, which was induced by TCDD, suggesting divergent regulation. Elovl5 null mice experience steatosis, which has been attributed to activation of SREBP-1c protein (Moon et al. 2008). MIX approached significant ($p=0.0619$) synergistic repression of Srebf1 consistent with less fat accumulation at 168 h compared to TCDD, which did not affect Srebf1 expression. In contrast, PCB153 repressed Srebf1 expression, consistent with the lack of lipid accumulation. Repression of SREBP-mediated lipogenesis in Zucker diabetic fatty rats is also associated with CAR/PXR-mediated over-expression of insulin induced genes (Insig1/2) (Takaishi et al. 2004; Roth et al. 2008). PCB153 and MIX induced Insig2, while TCDD down-regulated Insig2 at 4 h, consistent with the observed hepatic phenotypes.

Pla2g12a, a novel secretory phospholipase, which is involved in the digestion of dietary phospholipids, and the production of molecules that induce inflammatory responses (Gelb et al. 2000) was also synergistically induced by MIX. Although Pla2g12a induction may be linked to elevated free fatty acids, reports suggest it has weak catalytic activity and contributes little to increase cellular fatty acid release (Gelb et al. 2000; Murakami et al. 2003).

High doses of TCDD and dioxin-like chemicals cause feed refusal, body weight loss, and exhaustion of energy sources, collectively referred to as “wasting syndrome” (Viluksela et al. 1995). PCB153 is linked to increased glucose consumption in MCF-10A human non-tumorigenic mammary epithelial cells (Venkatesha et al. 2010). TCDD and MIX repression of the glucose metabolism genes, including glutamate oxaloacetate soluble 1, (Got1), glycerol-phosphate dehydrogenase 2, mitochondrial (Gpd2), and pyruvate dehydrogenase kinase, isoenzyme 1 (Pdk1), are consistent with the TCDD repression of gluconeogenesis in chick embryo hepatocytes and dioxin-mediated reversal of hyperglycemia in a diabetes rat model (Diani-Moore et al. 2010; Fried et al. 2010). MIX also repressed Got1 expression, but modeling did not confirm non-additive expression.

The lack of hepatocellular necrosis in PCB153-treated mice compared to TCDD and MIX, is consistent with reports of decreases in PCB153-mediated cell death in mouse hepatocytes

(Tharappel et al. 2002; Lu et al. 2004). In contrast, TCDD and MIX induced Tnfaip2 and Tnfaip8l1, members of the tumor necrosis factor (TNF)-signaling pathway, which mediate cell death and inflammation (Tracey and Cerami 1994). In addition, TCDD and MIX, but not PCB153, induced pro-apoptotic Bcl2l11and Htatip2 (Shi et al. 2008; Seitz et al. 2010).

TCPOBOP, a potent CAR ligand, also increased hepatic proliferation by 30–50% when co-treated with TCDD (Mitchell et al. 2010), suggesting TCDD synergizes with TCPOBOP to induce hyperplasia (Mitchell et al. 2010). MIX-induced hyperplasia is consistent with the induction of Myc, a transcription factor associated with cell proliferation, growth and metabolism (Dang 1999). Early response 3 (Ier3), which is anti-apoptotic and associated with cell proliferation (Wu 2003), is regulated by Myc, and was induced by TCDD and MIX, but not PCB153.

Histopathology also revealed PCB153 did not elicit inflammatory cell infiltration, unlike TCDD and MIX. The number of immune related genes increased following TCDD and MIX treatment, including major histocompatibility complex molecules H2-Eb1, H2-DMa, and H2-DMb1 (Gottstein et al. 2010). However, increases in the levels of these transcripts are not due to AhR-mediated expression but rather the coincident infiltration of immune cells.

MIX synergistically induced Serpinb6a, a serine protease inhibitor associated with inflammation and cell death (Scott et al. 2007). Serpinb6a is highly expressed by mast cells in all organs and may regulate endogenous β-tryptase in the cytoplasm, a biomarker of mast cell activation and mastocytosis immune response (Strik et al. 2004). Although PCB153 did not affect Serpinb6a expression, its induction by TCDD at later time points and synergistic induction by MIX was paralleled by the increased incidence of immune cell infiltration.

MIX also suppressed Dexi, a dexamethasone induced transcript that is regulated by PXR (Huss and Kasper 2000; Edgar et al. 2001) between 24 and 168 h. In contrast, Dexi was only transiently repressed by TCDD or PCB153 alone. Glucocorticoids, like dexamethasone, are linked to the suppression of inflammatory responses, partially by regulated expression of TNF (Noti et al. 2010). MIX approached significant ($p=0.0806$) synergistic suppression of Dexi, concomitant with histopathological findings indicating significant immune cell infiltration.

Dysferlin (Dysf), a transmembrane protein implicated in calcium-dependent sarcolemmal membrane repair, exhibited the most dramatic synergistic response following MIX treatment. Dysf-deficient skeletal muscles induce and activate key inflammasome adaptor components, including NACHT, LRR and PYD-containing proteins (Rawat et al. 2010). The C2 domains of dysferlin have lipid binding specificity, and facilitate interactions with lipid bilayer components including phosphatidylserine (PtdS), phosphatidylinositol 4-phosphate (PtdIns[4]P) and phosphatidylinositol 4,5-bisphosphate (PtdIns[4,5]P_2) in a calcium-dependent fashion (Boesze-Battaglia and Schimmel 1997; Di Paolo and De Camilli 2006; Therrien et al. 2009). Interestingly, deficiencies in phosphatidylcholine synthesis, another major membrane component, are linked to muscular dystrophy (Li et al. 2005). MIX elicited the most significant changes in hepatic architecture including cell size and number that may be linked to cellular membrane stress. Dysf induction by MIX during membrane injury may

lead to calcium-dependent interactions with PtdS and PtdIns to patch and repair membrane damage (Therrien et al. 2009).

In summary, we have used a “no-interaction” hypothesis to statistically determine departure from additivity in a dose-response study linking gene expression changes to phenotypic endpoints. PCB153 co-administration with TCDD elicited significant synergistic gene expression responses associated with increases in RLW, hepatic cell size and number, immune response and lipid accumulation in ovariectomized C57BL/6 mice at 24 h. Complementary dose-response studies at other time points are likely to identify additional non-additive interactions that can be phenotypically anchored to apical endpoints. Interestingly, our analysis did not identify examples of significant gene expression antagonism, likely due to insufficient power and modest levels of repression. Moreover, non-additive changes in protein, enzymatic activity and metabolite levels may not be reflected in microarray data (Borgert 2007). Consequently, the further development of predictive models that integrate pharmacokinetic and pharmacodynamic components from disparate data sets (e.g., microarray, proteomic, metabolomic) are required in order to further elucidate the effects of mixture composition on elicited toxic effects.

Supplementary Material

Refer to Web version on PubMed Central for supplementary material.

Acknowledgments

FUNDING: This work was supported by the National Institute of Environmental Health Sciences Superfund Basic Research Program (P42ES04911).

The authors thank Agnes Forgacs, Michelle Angrish and Suntae Kim for critically reviewing this manuscript.

References

Bannister R, Safe S. Synergistic interactions of 2,3,7,8-TCDD and 2,2′,4,4′,5,5′-hexachlorobiphenyl in C57BL/6J and DBA/2J mice: role of the Ah receptor. Toxicology. 1987; 44:159–169. [PubMed: 3031851]

Biegel L, Harris M, Davis D, Rosengren R, Safe L, Safe S. 2,2′,4,4′,5,5′-hexachlorobiphenyl as a 2,3,7,8-tetrachlorodibenzo-p-dioxin antagonist in C57BL/6J mice. Toxicol Appl Pharmacol. 1989; 97:561–571. [PubMed: 2558429]

Blumberg B, Evans RM. Orphan nuclear receptors--new ligands and new possibilities. Genes & development. 1998; 12:3149–3155. [PubMed: 9784489]

Boesze-Battaglia K, Schimmel R. Cell membrane lipid composition and distribution: implications for cell function and lessons learned from photoreceptors and platelets. J Exp Biol. 1997; 200:2927–2936. [PubMed: 9359876]

Borgert CJ. Predicting interactions from mechanistic information: can omic data validate theories? Toxicol Appl Pharmacol. 2007; 223:114–120. [PubMed: 17306318]

Borgert CJ, Price B, Wells CS, Simon GS. Evaluating chemical interaction studies for mixture risk assessment. Human and Ecological Risk Assessment. 2001; 7:259–305.

Boverhof DR, Burgoon LD, Tashiro C, Chittim B, Harkema JR, Jump DB, Zacharewski TR. Temporal and dose-dependent hepatic gene expression patterns in mice provide new insights into TCDD-Mediated hepatotoxicity. Toxicol Sci. 2005; 85:1048–1063. [PubMed: 15800033]

Boverhof DR, Burgoon LD, Tashiro C, Sharratt B, Chittim B, Harkema JR, Mendrick DL, Zacharewski TR. Comparative toxicogenomic analysis of the hepatotoxic effects of TCDD in Sprague Dawley rats and C57BL/6 mice. Toxicol Sci. 2006; 94:398–416. [PubMed: 16960034]

Burgoon LD, Eckel-Passow JE, Gennings C, Boverhof DR, Burt JW, Fong CJ, Zacharewski TR. Protocols for the assurance of microarray data quality and process control. Nucleic Acids Res. 2005; 33:e172. [PubMed: 16272462]

Burgoon LD, Zacharewski TR. dbZach toxicogenomic information management system. Pharmacogenomics. 2007; 8:287–291. [PubMed: 17324117]

Commoner B, Shapiro K, Webster T. The Origin and Health Risks of PCDD and PCDF. Waste Management & Research. 1987; 5:327–346.

Craft ES, DeVito MJ, Crofton KM. Comparative responsiveness of hypothyroxinemia and hepatic enzyme induction in Long-Evans rats versus C57BL/6J mice exposed to TCDD-like and phenobarbital-like polychlorinated biphenyl congeners. Toxicol Sci. 2002; 68:372–380. [PubMed: 12151633]

Dang CV. c-Myc target genes involved in cell growth, apoptosis, and metabolism. Molecular and cellular biology. 1999; 19:1–11. [PubMed: 9858526]

De Jongh J, DeVito M, Diliberto J, Van den Berg M, Birnbaum L. The effects of 2,2′,4,4′,5,5′-hexachlorobiphenyl cotreatment on the disposition of 2,3,7,8-tetrachlorodibenzo-p-dioxin in mice. Toxicol Lett. 1995; 80:131–137. [PubMed: 7482580]

De Jongh J, Wondergem F, Seinen W, Van den Berg M. Toxicokinetic interactions in the liver of the C57BL/6J mouse after administration of a single oral dose of a binary mixture of some PCBs. Chemosphere. 1992; 25:1165–1170.

Denison MS, Heath-Pagliuso S. The Ah receptor: a regulator of the biochemical and toxicological actions of structurally diverse chemicals. Bull Environ Contam Toxicol. 1998; 61:557–568. [PubMed: 9841714]

Denison MS, Pandini A, Nagy SR, Baldwin EP, Bonati L. Ligand binding and activation of the Ah receptor. Chemico-biological interactions. 2002; 141:3–24. [PubMed: 12213382]

Dennis G Jr, Sherman BT, Hosack DA, Yang J, Gao W, Lane HC, Lempicki RA. DAVID: Database for Annotation, Visualization, and Integrated Discovery. Genome biology. 2003; 4:P3. [PubMed: 12734009]

Dere E, Forgacs AL, Zacharewski TR, Burgoon LD. Genome-wide computational analysis of dioxin response element location and distribution in the human, mouse and rat genomes. Chem Res Toxicol. 2011a; 24:494–504. [PubMed: 21370876]

Dere E, Lee AW, Burgoon LD, Zacharewski TR. Differences in TCDD-elicited gene expression profiles in human HepG2, mouse Hepa1c1c7 and rat H4IIE hepatoma cells. BMC Genomics. 2011b; 12:193. [PubMed: 21496263]

DeVito MJ, Ross DG, Dupuy AE Jr, Ferrario J, McDaniel D, Birnbaum LS. Dose-response relationships for disposition and hepatic sequestration of polyhalogenated dibenzo-p-dioxins, dibenzofurans, and biphenyls following subchronic treatment in mice. Toxicol Sci. 1998; 46:223–234. [PubMed: 10048125]

Di Paolo G, De Camilli P. Phosphoinositides in cell regulation and membrane dynamics. Nature. 2006; 443:651–657. [PubMed: 17035995]

Diani-Moore S, Ram P, Li X, Mondal P, Youn DY, Sauve AA, Rifkind AB. Identification of the aryl hydrocarbon receptor target gene Tiparp as a mediator of suppression of hepatic gluconeogenesis by 2,3,7,8-tetrachlorodibenzo-p-dioxin and of nicotinamide as a corrective agent for this effect. J Biol Chem. 2010; 285:38801–38810. [PubMed: 20876576]

Diliberto JJ, Burgin DE, Birnbaum LS. Effects of CYP1A2 on disposition of 2,3,7, 8-tetrachlorodibenzo-p-dioxin, 2,3,4,7,8-pentachlorodibenzofuran, and 2,2′,4,4′,5,5′-hexachlorobiphenyl in CYP1A2 knockout and parental (C57BL/6N and 129/Sv) strains of mice. Toxicol Appl Pharmacol. 1999; 159:52–64. [PubMed: 10448125]

Eckel JE, Gennings C, Chinchilli VM, Burgoon LD, Zacharewski TR. Empirical bayes gene screening tool for time-course or dose-response microarray data. J Biopharm Stat. 2004; 14:647–670. [PubMed: 15468757]

Eckel JE, Gennings C, Therneau TM, Burgoon LD, Boverhof DR, Zacharewski TR. Normalization of two-channel microarray experiments: a semiparametric approach. Bioinformatics. 2005; 21:1078–1083. [PubMed: 15513988]

Edgar AJ, Birks EJ, Yacoub MH, Polak JM. Cloning of dexamethasone-induced transcript: a novel glucocorticoid-induced gene that is upregulated in emphysema. Am J Respir Cell Mol Biol. 2001; 25:119–124. [PubMed: 11472984]

FDA. Dose Selection for Carcinogenicity Studies. 2008:1–10.

Fried KW, Guo GL, Esterly N, Kong B, Rozman KK. 2,3,7,8-tetrachlorodibenzo-p-dioxin (TCDD) reverses hyperglycemia in a type II diabetes mellitus rat model by a mechanism unrelated to PPAR gamma. Drug Chem Toxicol. 2010; 33:261–268. [PubMed: 20429801]

Gelb MH, Valentin E, Ghomashchi F, Lazdunski M, Lambeau G. Cloning and recombinant expression of a structurally novel human secreted phospholipase A2. J Biol Chem. 2000; 275:39823–39826. [PubMed: 11031251]

Gennings C, Carter WH, Campain JA, Bae DS, Yang RSH. Statistical analysis of interactive cytotoxicity in human epidermal keratinocytes following exposure to a mixture of four metals. J Agric Biol Environ Stat. 2002; 7:58–73.

Gottstein B, Wittwer M, Schild M, Merli M, Leib SL, Muller N, Muller J, Jaggi R. Hepatic gene expression profile in mice perorally infected with Echinococcus multilocularis eggs. PLoS One. 2010; 5:e9779. [PubMed: 20368974]

Greco D, Kotronen A, Westerbacka J, Puig O, Arkkila P, Kiviluoto T, Laitinen S, Kolak M, Fisher RM, Hamsten A, Auvinen P, Yki-Jarvinen H. Gene expression in human NAFLD. Am J Physiol Gastrointest Liver Physiol. 2008; 294:G1281–1287. [PubMed: 18388185]

Honkakoski P, Sueyoshi T, Negishi M. Drug-activated nuclear receptors CAR and PXR. Annals of medicine. 2003; 35:172–182. [PubMed: 12822739]

Huss JM, Kasper CB. Two-stage glucocorticoid induction of CYP3A23 through both the glucocorticoid and pregnane X receptors. Mol Pharmacol. 2000; 58:48–57. [PubMed: 10860926]

Kimbrough RD. Polychlorinated biphenyls (PCBs) and human health: an update. Crit Rev Toxicol. 1995; 25:133–163. [PubMed: 7612174]

Klaassen CD, Reisman SA. Nrf2 the rescue: effects of the antioxidative/electrophilic response on the liver. Toxicol Appl Pharmacol. 2010; 244:57–65. [PubMed: 20122946]

Knerr S, Schrenk D. Carcinogenicity of “non-dioxinlike” polychlorinated biphenyls. Crit Rev Toxicol. 2006; 36:663–694. [PubMed: 17050081]

Kopec AK, Boverhof DR, Burgoon LD, Ibrahim-Aibo D, Harkema JR, Tashiro C, Chittim B, Zacharewski TR. Comparative Toxicogenomic Examination of the Hepatic Effects of PCB126 and TCDD in Immature, Ovariectomized C57BL/6 Mice. Toxicol Sci. 2008; 102:61–75. [PubMed: 18042819]

Kopec AK, Burgoon LD, Ibrahim-Aibo D, Burg AR, Lee AW, Tashiro C, Potter D, Sharratt B, Harkema JR, Rowlands JC, Budinsky RA, Zacharewski TR. Automated Dose-Response Analysis and Comparative Toxicogenomic Evaluation of the Hepatic Effects Elicited by TCDD, TCDF and PCB126 in C57BL/6 Mice. Toxicol Sci. 2010a; 118:286–297. [PubMed: 20702594]

Kopec AK, Burgoon LD, Ibrahim-Aibo D, Mets BD, Tashiro C, Potter D, Sharratt B, Harkema JR, Zacharewski TR. PCB153-elicited hepatic responses in the immature, ovariectomized C57BL/6 mice: Comparative toxicogenomic effects of dioxin and non-dioxin-like ligands. Toxicol Appl Pharmacol. 2010b; 243:359–371. [PubMed: 20005886]

Lee JH, Wada T, Febbraio M, He J, Matsubara T, Lee MJ, Gonzalez FJ, Xie W. A Novel Role for the Dioxin Receptor in Fatty Acid Metabolism and Hepatic Steatosis. Gastroenterology. 2010; 139:653–663. [PubMed: 20303349]

Lemaire G, Benod C, Nahoum V, Pillon A, Boussioux AM, Guichou JF, Subra G, Pascussi JM, Bourguet W, Chavanieu A, Balaguer P. Discovery of a highly active ligand of human pregnane x receptor: a case study from pharmacophore modeling and virtual screening to “in vivo” biological activity. Mol Pharmacol. 2007; 72:572–581. [PubMed: 17573484]

Li Z, Agellon LB, Vance DE. Phosphatidylcholine homeostasis and liver failure. J Biol Chem. 2005; 280:37798–37802. [PubMed: 16144842]

Liu MJ, Takahashi Y, Wada T, He J, Gao J, Tian Y, Li S, Xie W. The aldo-keto reductase Akr1b7 gene is a common transcriptional target of xenobiotic receptors pregnane X receptor and constitutive androstane receptor. Mol Pharmacol. 2009; 76:604–611. [PubMed: 19542321]

Lu Z, Lee EY, Robertson LW, Glauert HP, Spear BT. Effect of 2,2′,4,4′,5,5′-hexachlorobiphenyl (PCB-153) on hepatocyte proliferation and apoptosis in mice deficient in the p50 subunit of the transcription factor NF-kappaB. Toxicol Sci. 2004; 81:35–42. [PubMed: 15201435]

Ma Q, Kinneer K, Bi Y, Chan JY, Kan YW. Induction of murine NAD(P)H:quinone oxidoreductase by 2,3,7,8-tetrachlorodibenzo-p-dioxin requires the CNC (cap 'n' collar) basic leucine zipper transcription factor Nrf2 (nuclear factor erythroid 2-related factor 2): cross-interaction between AhR (aryl hydrocarbon receptor) and Nrf2 signal transduction. The Biochemical journal. 2004; 377:205–213. [PubMed: 14510636]

Maglich JM, Stoltz CM, Goodwin B, Hawkins-Brown D, Moore JT, Kliewer SA. Nuclear pregnane x receptor and constitutive androstane receptor regulate overlapping but distinct sets of genes involved in xenobiotic detoxification. Mol Pharmacol. 2002; 62:638–646. [PubMed: 12181440]

Masahiko N, Honkakoski P. Induction of drug metabolism by nuclear receptor CAR: molecular mechanisms and implications for drug research. Eur J Pharm Sci. 2000; 11:259–264. [PubMed: 11033069]

Mason G, Safe S. Synthesis, biologic and toxic effects of the major 2,3,7,8-tetrachlorodibenzo-p-dioxin metabolites in the rat. Toxicology. 1986; 41:153–159. [PubMed: 3764940]

Matsumoto K, Endo S, Ishikura S, Matsunaga T, Tajima K, El-Kabbani O, Hara A. Enzymatic properties of a member (AKR1C20) of the aldo-keto reductase family. Biological & pharmaceutical bulletin. 2006; 29:539–542. [PubMed: 16508162]

Mitchell KA, Wilson SR, Elferink CJ. The activated aryl hydrocarbon receptor synergizes mitogen-induced murine liver hyperplasia. Toxicology. 2010; 276:103–109. [PubMed: 20637255]

Moon YA, Hammer RE, Horton JD. Deletion of ELOVL5 leads to fatty liver through activation of SREBP-1c in mice. Journal of lipid research. 2008; 50:412–423. [PubMed: 18838740]

Mullin MD, Pochini CM, McCrindle S, Romkes M, Safe SH, Safe LM. High-resolution PCB analysis: synthesis and chromatographic properties of all 209 PCB congeners. Environ Set Technol. 1984; 18:468–476.

Murakami M, Masuda S, Shimbara S, Bezzine S, Lazdunski M, Lambeau G, Gelb MH, Matsukura S, Kokubu F, Adachi M, Kudo I. Cellular arachidonate-releasing function of novel classes of secretory phospholipase A2s (groups III and XII). J Biol Chem. 2003; 278:10657–10667. [PubMed: 12522102]

Nebert DW, Petersen DD, Fornace AJ Jr. Cellular responses to oxidative stress: the [Ah] gene battery as a paradigm. Environ Health Perspect. 1990; 88:13–25. [PubMed: 2272308]

Nebert DW, Roe AL, Dieter MZ, Solis WA, Yang Y, Dalton TP. Role of the aromatic hydrocarbon receptor and [Ah] gene battery in the oxidative stress response, cell cycle control, and apoptosis. Biochem Pharmacol. 2000; 59:65–85. [PubMed: 10605936]

Noti M, Corazza N, Mueller C, Berger B, Brunner T. TNF suppresses acute intestinal inflammation by inducing local glucocorticoid synthesis. The Journal of experimental medicine. 2010; 207:1057–1066. [PubMed: 20439544]

NTP. NTP technical report on the toxicology and carcinogenesis studies of 2, 2 ′,4,4′,5,5′-hexachlorobiphenyl (PCB 153) (CAS No. 35065-27-1) in female Harlan Sprague-Dawley rats (Gavage studies). Natl Toxicol Program Tech Rep Ser 4–168. 2006a

NTP. NTP technical report on the toxicology and carcinogenesis studies of 2, 3,7,8-tetrachlorodibenzo-p-dioxin (TCDD) (CAS No. 1746-01-6) in female Harlan Sprague-Dawley rats (Gavage Studies). Natl Toxicol Program Tech Rep Ser 4–232. 2006b

NTP. NTP Toxicology and Carcinogenesis Studies of 3, 3′,4,4′,5-pentachlorobiphenyl (PCB 126) (CAS No. 57465-28-8) in Female Harlan Sprague-Dawley Rats (Gavage Studies). National Toxicology Program technical report series 4–246. 2006c

NTP. NTP Toxicology and Carcinogenesis Studies of a Binary Mixture of 3, 3′,4,4′,5-Pentachlorobiphenyl (PCB 126) (CAS No. 57465-28-8) and 2,2′,4,4′,5,5′-Hexachlorobiphenyl (PCB 153) (CAS No. 35065-27-1) in Female Harlan Sprague-Dawley Rats (Gavage Studies). National Toxicology Program technical report series 1–258. 2006d

Park JW, Mieyal JJ, Rhee SG, Chock PB. Deglutathionylation of 2-Cys peroxiredoxin is specifically catalyzed by sulfiredoxin. J Biol Chem. 2009; 284:23364–23374. [PubMed: 19561357]

Phillips JM, Burgoon LD, Goodman JI. Phenobarbital (PB) Elicits Unique, Early Changes in the Expression of Hepatic Genes That Affect Critical Pathways in Tumor-Prone B6C3F1 Mice. Toxicol Sci. 2009; 109:193–205. [PubMed: 19270015]

Poland A, Glover E. Studies on the mechanism of toxicity of the chlorinated dibenzo-p-dioxins. Environ Health Perspect. 1973; 5:245–251. [PubMed: 4752907]

Poland A, Knutson JC. 2,3,7,8-tetrachlorodibenzo-p-dioxin and related halogenated aromatic hydrocarbons: examination of the mechanism of toxicity. Annu Rev Pharmacol Toxicol. 1982; 22:517–554. [PubMed: 6282188]

Rawat R, Cohen TV, Ampong B, Francia D, Henriques-Pons A, Hoffman EP, Nagaraju K. Inflammasome up-regulation and activation in dysferlin-deficient skeletal muscle. Am J Pathol. 2010; 176:2891–2900. [PubMed: 20413686]

Roth A, Looser R, Kaufmann M, Blattler SM, Rencurel F, Huang W, Moore DD, Meyer UA. Regulatory cross-talk between drug metabolism and lipid homeostasis: constitutive androstane receptor and pregnane X receptor increase Insig-1 expression. Mol Pharmacol. 2008; 73:1282–1289. [PubMed: 18187584]

Safe S. Polychlorinated biphenyls (PCBs), dibenzo-p-dioxins (PCDDs), dibenzofurans (PCDFs), and related compounds: environmental and mechanistic considerations which support the development of toxic equivalency factors (TEFs). Crit Rev Toxicol. 1990; 21:51–88. [PubMed: 2124811]

Safe S. Limitations of the toxic equivalency factor approach for risk assessment of TCDD and related compounds. Teratog Carcinog Mutagen. 1997; 17:285–304. [PubMed: 9508738]

Safe S. Molecular biology of the Ah receptor and its role in carcinogenesis. Toxicol Lett. 2001; 120:1–7. [PubMed: 11323156]

Safe S, Robertson LW, Safe L, Parkinson A, Bandiera S, Sawyer T, Campbell MA. Halogenated biphenyls: molecular toxicology. Can J Physiol Pharmacol. 1982; 60:1057–1064. [PubMed: 6812934]

Safe SH. Polychlorinated biphenyls (PCBs): environmental impact, biochemical and toxic responses, and implications for risk assessment. Crit Rev Toxicol. 1994; 24:87–149. [PubMed: 8037844]

Schecter A, Stanley J, Boggess K, Masuda Y, Mes J, Wolff M, Furst P, Furst C, Wilson-Yang K, Chisholm B. Polychlorinated biphenyl levels in the tissues of exposed and nonexposed humans. Environ Health Perspect. 1994; 102(Suppl 1):149–158. [PubMed: 8187704]

Scott FL, Sun J, Whisstock JC, Kato K, Bird PI. SerpinB6 is an inhibitor of kallikrein-8 in keratinocytes. Journal of biochemistry. 2007; 142:435–442. [PubMed: 17761692]

Seitz SJ, Schleithoff ES, Koch A, Schuster A, Teufel A, Staib F, Stremmel W, Melino G, Krammer PH, Schilling T, Muller M. Chemotherapy-induced apoptosis in hepatocellular carcinoma involves the p53 family and is mediated via the extrinsic and the intrinsic pathway. Int J Cancer. 2010; 126:2049–2066. [PubMed: 19711344]

Sheehan, DC.; Hrapchak, BB. Theory and Practice of Histotechnology. Mosby; St. Louis: 1980.

Shi M, Yan SG, Xie ST, Wang HN. Tip30-induced apoptosis requires translocation of Bax and involves mitochondrial release of cytochrome c and Smac/DIABLO in hepatocellular carcinoma cells. Biochimica et biophysica acta. 2008; 1783:263–274. [PubMed: 17997990]

Singh A, Ling G, Suhasini AN, Zhang P, Yamamoto M, Navas-Acien A, Cosgrove G, Tuder RM, Kensler TW, Watson WH, Biswal S. Nrf2-dependent sulfiredoxin-1 expression protects against cigarette smoke-induced oxidative stress in lungs. Free radical biology & medicine. 2009; 46:376–386. [PubMed: 19027064]

Staal YC, Hebels DG, van Herwijnen MH, Gottschalk RW, van Schooten FJ, van Delft JH. Binary PAH mixtures cause additive or antagonistic effects on gene expression but synergistic effects on DNA adduct formation. Carcinogenesis. 2007; 28:2632–2640. [PubMed: 17690111]

Strik MC, Wolbink A, Wouters D, Bladergroen BA, Verlaan AR, van Houdt IS, Hijlkema S, Hack CE, Kummer JA. Intracellular serpin SERPINB6 (PI6) is abundantly expressed by human mast cells and forms complexes with beta-tryptase monomers. Blood. 2004; 103:2710–2717. [PubMed: 14670919]

Suh J, Kang JS, Yang KH, Kaminski NE. Antagonism of aryl hydrocarbon receptor-dependent induction of CYP1A1 and inhibition of IgM expression by di-ortho-substituted polychlorinated biphenyls. Toxicol Appl Pharmacol. 2003; 187:11–21. [PubMed: 12628580]

Sun YV, Boverhof DR, Burgoon LD, Fielden MR, Zacharewski TR. Comparative analysis of dioxin response elements in human, mouse and rat genomic sequences. Nucleic Acids Res. 2004; 32:4512–4523. [PubMed: 15328365]

Tabb MM, Kholodovych V, Grun F, Zhou C, Welsh WJ, Blumberg B. Highly chlorinated PCBs inhibit the human xenobiotic response mediated by the steroid and xenobiotic receptor (SXR). Environ Health Perspect. 2004; 112:163–169. [PubMed: 14754570]

Takaishi K, Duplomb L, Wang MY, Li J, Unger RH. Hepatic insig-1 or -2 overexpression reduces lipogenesis in obese Zucker diabetic fatty rats and in fasted/refed normal rats. Proc Natl Acad Sci U S A. 2004; 101:7106–7111. [PubMed: 15096598]

Tharappel JC, Lee EY, Robertson LW, Spear BT, Glauert HP. Regulation of cell proliferation, apoptosis, and transcription factor activities during the promotion of liver carcinogenesis by polychlorinated biphenyls. Toxicol Appl Pharmacol. 2002; 179:172–184. [PubMed: 11906247]

Therrien C, Di Fulvio S, Pickles S, Sinnreich M. Characterization of lipid binding specificities of dysferlin C2 domains reveals novel interactions with phosphoinositides. Biochemistry. 2009; 48:2377–2384. [PubMed: 19253956]

Tijet N, Boutros PC, Moffat ID, Okey AB, Tuomisto J, Pohjanvirta R. Aryl hydrocarbon receptor regulates distinct dioxin-dependent and dioxin-independent gene batteries. Mol Pharmacol. 2006; 69:140–153. [PubMed: 16214954]

Tracey KJ, Cerami A. Tumor necrosis factor: a pleiotropic cytokine and therapeutic target. Annu Rev Med. 1994; 45:491–503. [PubMed: 8198398]

van Birgelen AP, Fase KM, van der Kolk J, Poiger H, Brouwer A, Seinen W, van den Berg M. Synergistic effect of 2,2′,4,4′,5,5′-hexachlorobiphenyl and 2,3,7,8-tetrachlorodibenzo-p-dioxin on hepatic porphyrin levels in the rat. Environ Health Perspect. 1996a; 104:550–557. [PubMed: 8743444]

van Birgelen AP, Ross DG, DeVito MJ, Birnbaum LS. Interactive effects between 2,3,7,8-tetrachlorodibenzo-p-dioxin and 2,2′,4,4′,5,5′-hexachlorobiphenyl in female B6C3F1 mice: tissue distribution and tissue-specific enzyme induction. Fundam Appl Toxicol. 1996b; 34:118–131. [PubMed: 8937899]

Van den Berg M, Birnbaum LS, Denison M, De Vito M, Farland W, Feeley M, Fiedler H, Hakansson H, Hanberg A, Haws L, Rose M, Safe S, Schrenk D, Tohyama C, Tritscher A, Tuomisto J, Tysklind M, Walker N, Peterson RE. The 2005 World Health Organization reevaluation of human and Mammalian toxic equivalency factors for dioxins and dioxin-like compounds. Toxicol Sci. 2006; 93:223–241. [PubMed: 16829543]

Van der Kolk J, van Birgelen AP, Poiger H, Schlatter C. Interactions of 2,2′,4,4′,5,5′-hexachlorobiphenyl and 2,3,7,8-tetrachlorodibenzo-p-dioxin in a subchronic feeding study in the rat. Chemosphere. 1992; 25:2023–2027.

Vandesompele J, De Preter K, Pattyn F, Poppe B, Van Roy N, De Paepe A, Speleman F. Accurate normalization of real-time quantitative RT-PCR data by geometric averaging of multiple internal control genes. Genome biology. 2002; 3:RESEARCH0034. [PubMed: 12184808]

Venkatesha VA, Kalen AL, Sarsour EH, Goswami PC. PCB-153 exposure coordinates cell cycle progression and cellular metabolism in human mammary epithelial cells. Toxicol Lett. 2010; 196:110–116. [PubMed: 20394812]

Viluksela M, Stahl BU, Rozman KK. Tissue-specific effects of 2,3,7,8-Tetrachlorodibenzo-p-dioxin (TCDD) on the activity of phosphoenolpyruvate carboxykinase (PEPCK) in rats. Toxicol Appl Pharmacol. 1995; 135:308–315. [PubMed: 8545841]

Wu MX. Roles of the stress-induced gene IEX-1 in regulation of cell death and oncogenesis. Apoptosis. 2003; 8:11–18. [PubMed: 12510147]

Yeager RL, Reisman SA, Aleksunes LM, Klaassen CD. Introducing the “TCDD-inducible AhR-Nrf2 gene battery”. Toxicol Sci. 2009; 111:238–246. [PubMed: 19474220]

Zhai Y, Wada T, Zhang B, Khadem S, Ren S, Kuruba R, Li S, Xie W. A functional cross-talk between liver X receptor-alpha and constitutive androstane receptor links lipogenesis and xenobiotic responses. Mol Pharmacol. 2010; 78:666–674. [PubMed: 20592274]

Zhao F, Mayura K, Harper N, Safe SH, Phillips TD. Inhibition of 3,3′,4,4′,5-pentachlorobiphenyl-induced fetal cleft palate and immunotoxicity in C57BL/6 mice by 2,2′,4,4′,5,5′-hexachlorobiphenyl. Chemosphere. 1997; 34:1605–1613. [PubMed: 9134691]

Highlights

- MIX (TCDD:PCB153 at 1:10,000 ratio) exposure leads to non-additive gene expression.
- MIX-induced liver weights are significantly greater relative to single chemicals.
- MIX exposure leads to potentiation of hepatic PCB153 levels compared to TCDD.
- MIX synergistically induces expression of Nqo1, Dysf, Pla2g12a, Serpinb6a, and Srxn1.
- Non-additive gene expression supports putative non-additive phenotypic responses.

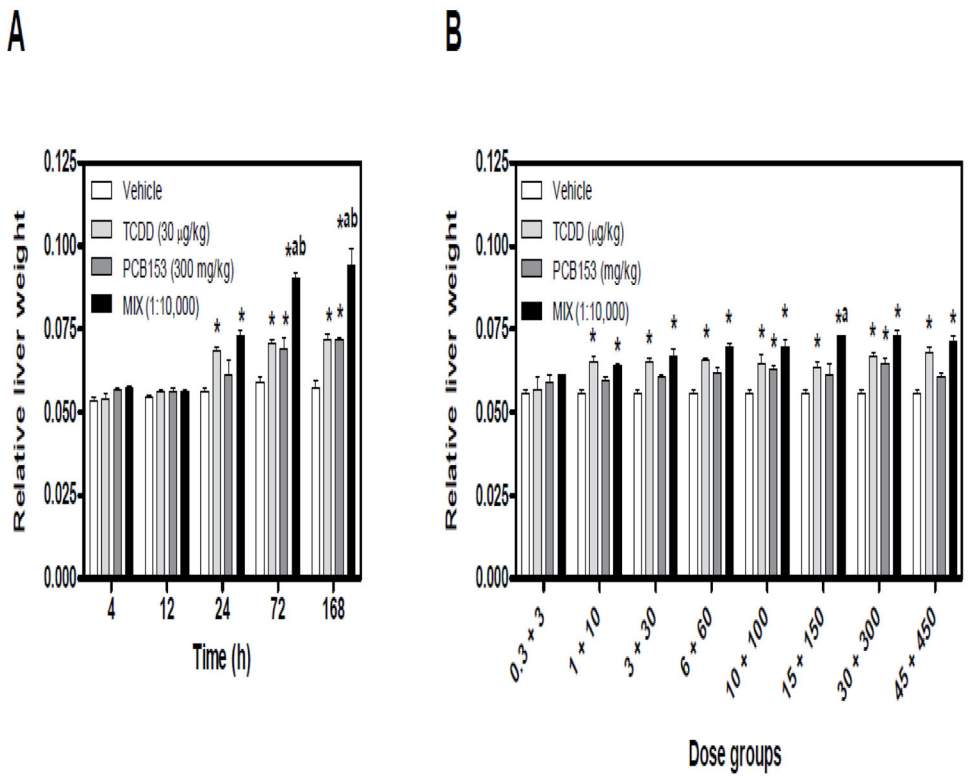

Figure 1.

Temporal and dose-dependent changes in the relative liver weight following exposure to TCDD, PCB153, and MIX. (**A)** In the time course study, 30 µg/kg TCDD + 300 mg/kg PCB153 were co-administered (MIX, 1:10,000 TCDD to PCB153). (**B)** In the 24 h dose-response, MIX (µg/kg TCDD + mg/kg PCB153) was administered at 1:10,000 ratio of TCDD to PCB153, respectively. Results are displayed as mean ± standard error (SE) for 5 independent replicates. Data were analyzed by analysis of variance (ANOVA) followed by Tukey's *post hoc* test: *$p<0.05$ vs. vehicle, $^{a}p<0.05$ vs. PCB153 and $^{b}p<0.05$ vs. TCDD. Time course increases in relative liver weight induced by individual TCDD and PCB153 treatments are from Kopec et al. (2010b).

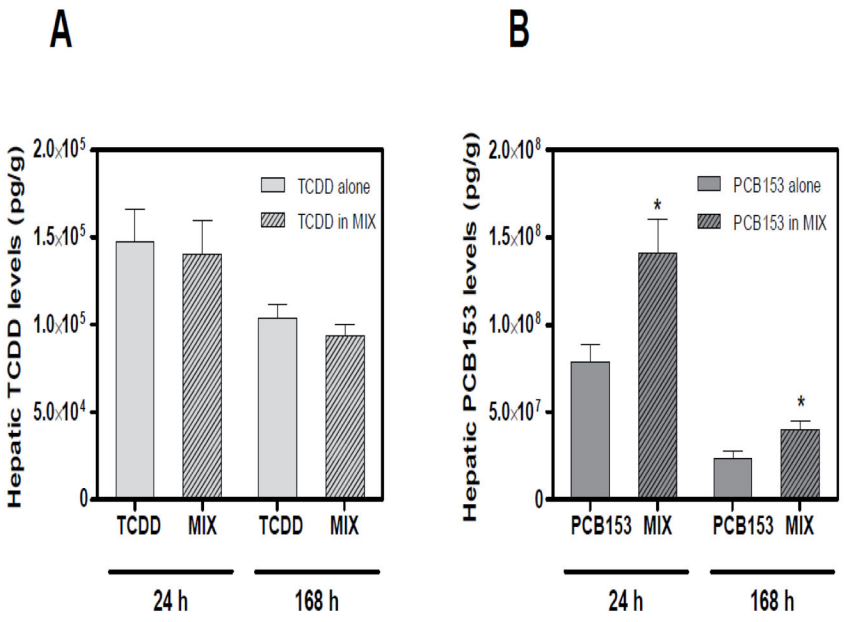

Figure 2.

Hepatic **(A)** TCDD and **(B)** PCB153 tissue levels per g liver wet weight measured by HRGC-HRMS (Kopec et al. 2010b). PCB153 levels were potentiated following co-administration with TCDD (in MIX) at 24 and 168 h. However no changes in TCDD hepatic levels were detected following co-treatment with PCB153 (in MIX). Results are displayed as mean ± SE for 3 independent replicates. Data were analyzed by ANOVA followed by Tukey's *post hoc* test: *$p<0.05$ vs. time-matched PCB153 levels alone.

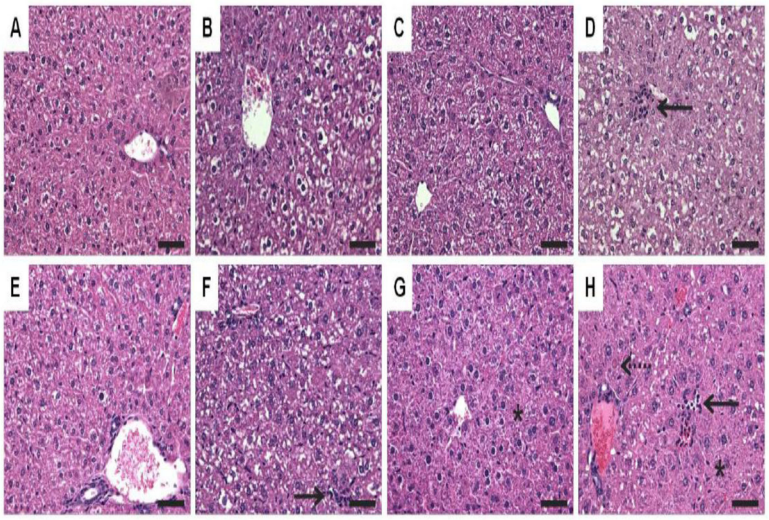

Figure 3.

Standard hematoxylin and eosin staining of liver sections at 24 (top panel: A–D) and 168 h (bottom panel: E–H). **(A&E)** Sesame oil elicited minimal vacuolization. **(B&F)** 30 μg/kg TCDD elicited vacuolization and inflammation (solid arrow). **(C&G)** 300 mg/kg PCB153 resulted in minimal vacuolization and hypertrophy (asterisk). **(D&H)** MIX resulted in vacuolization, inflammation (solid arrow), hypertrophy (asterisk) and necrosis (dashed arrow). Bars = 50 μm.

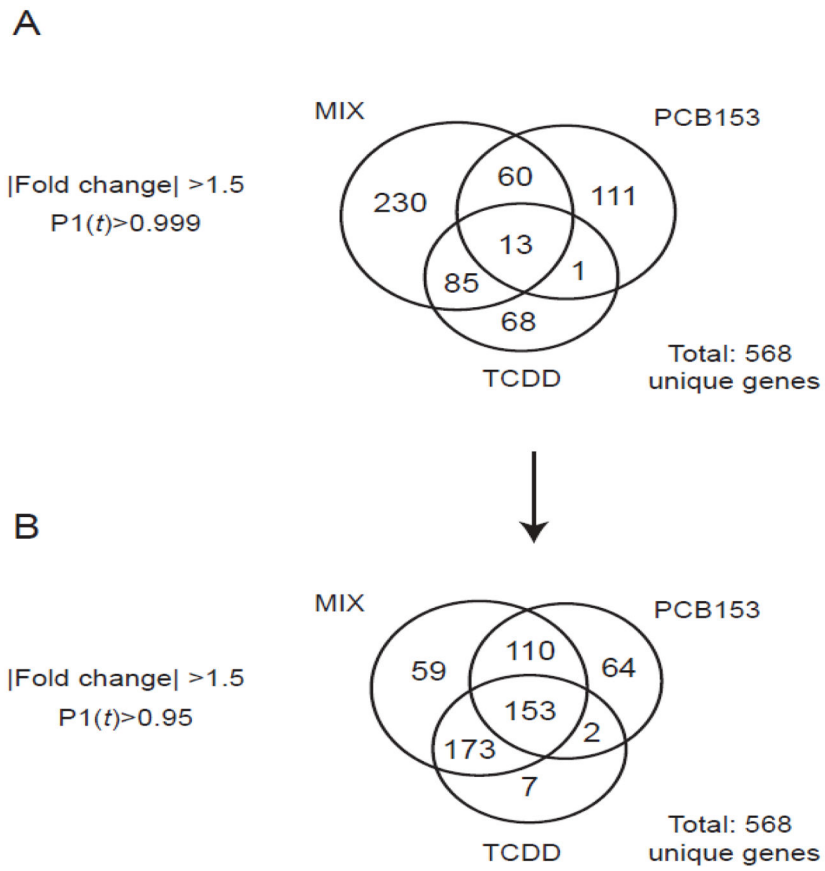

Figure 4.

Temporal microarray data sets for 30 μg/kg TCDD, 300 mg/kg PCB153 (Kopec et al. 2010b), and MIX (1:10,000 TCDD:PCB153) groups were compared using **(A)** stringent (|fold change|>1.5, P1(t)>0.999) and **(B)** relaxed (|fold change|>1.5, P1(t)>0.95) selection criteria. Numbers in the Venn diagram represent unique genes.

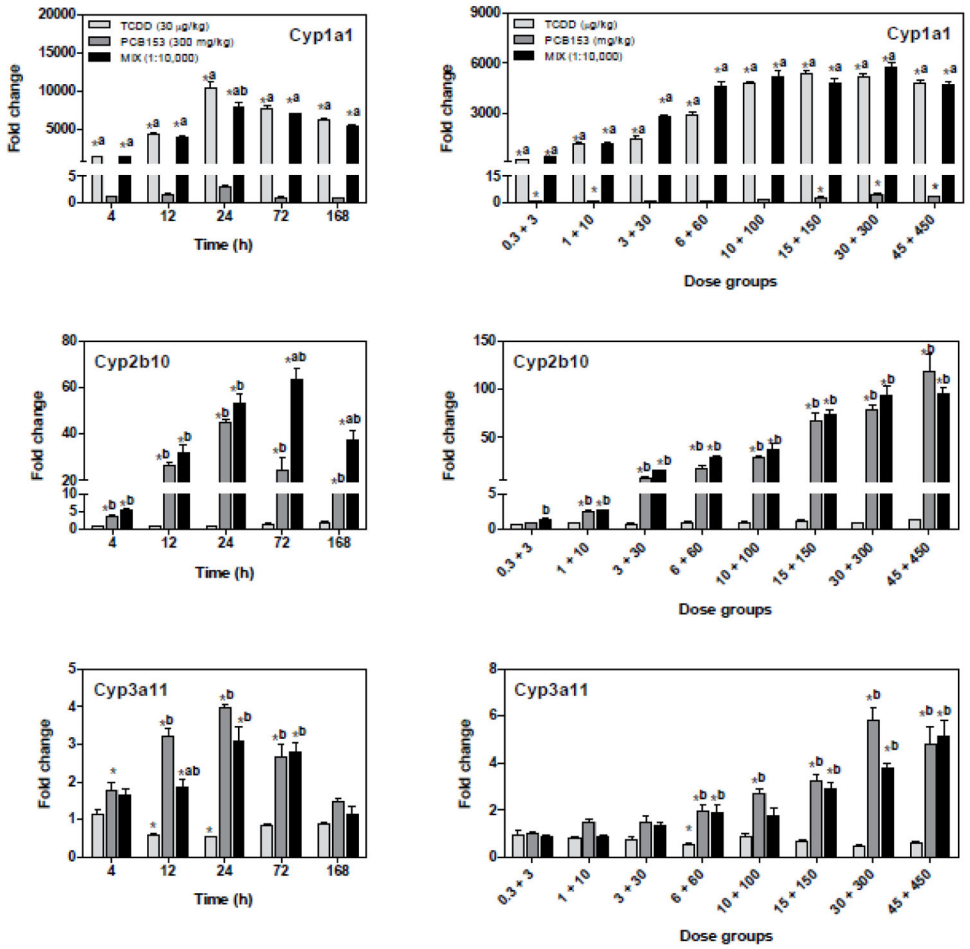

Figure 5.

QRTPCR verification of AhR, CAR, and PXR-regulated genes. TCDD induced Cyp1a1 (AhR), while PCB153 induced Cyp2b10 and Cyp3a11 (CAR/PXR), and MIX induced all three genes. All fold changes were calculated relative to time-matched vehicle controls. The genes are represented by their official gene symbols. Results are displayed as mean ± SE for 5 independent replicates. Data were analyzed by ANOVA followed by Tukey's *post hoc* test: *$p<0.05$ vs. time-matched vehicle, $^{a}p<0.05$ vs. PCB153 and $^{b}p<0.05$ vs. TCDD. TCDD and PCB153 temporal data are from Kopec et al. (2010b).

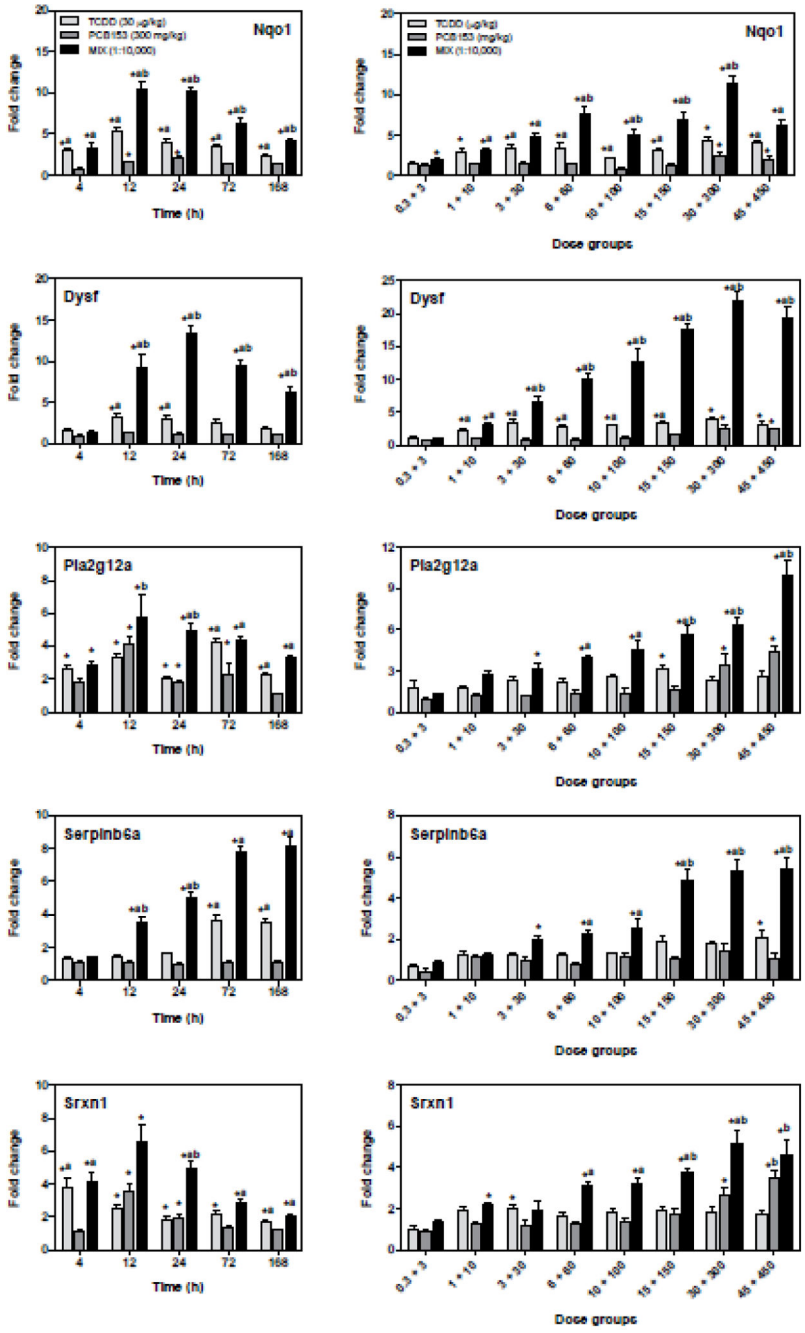

Figure 6.

Temporal and dose-dependent QRTPCR verification of putative non-additive genes. Genes exhibiting putative non-additive interactions initially identified in the time course study were verified by QRTPCR in the time course study and 24 h dose-response study. The genes are represented by their official gene symbols. Results are displayed as mean ± SE for 5 independent replicates. Data were analyzed by ANOVA followed by Tukey's *post hoc* test: *$p<0.05$ vs. time-matched vehicle, $^{a}p<0.05$ vs. PCB153 and $^{b}p<0.05$ vs. TCDD.

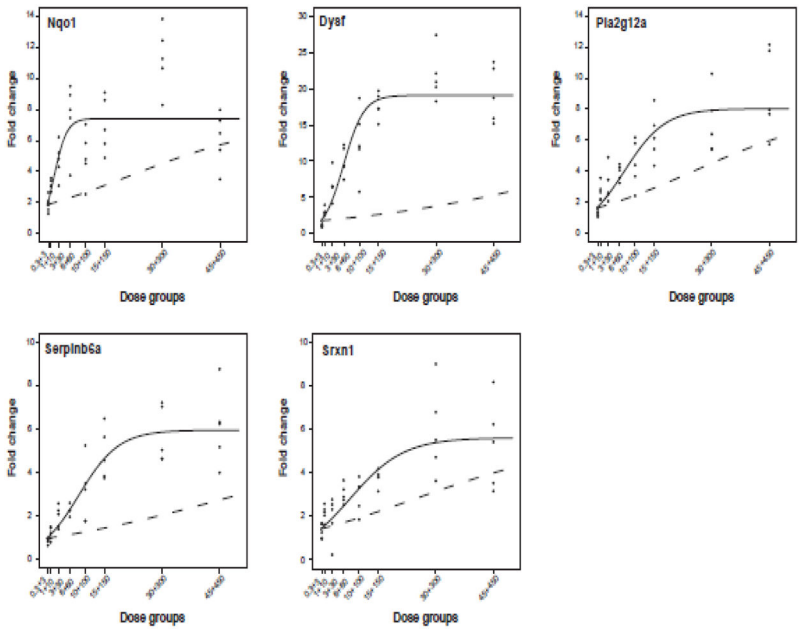

Figure 7.

Non-linear logistic modeling of QRTPCR dose-response data. Graphs depict the additive model (dashed line) generated using TCDD and PCB153 data and the mixture model (solid line) fitted using MIX data (black dots). MIX data for Nqo1, Dysf, Pla2g12a, Serpinb6a, and Srxn1 fit the mixture model better than the additivity model, indicating a statistically significant ($p<0.0001$) synergistic interaction.

Table 1

GC-MS analysis of fatty acid composition.

Time (h)	Treatment	SFA	MUFA	n3 PUFA	n6 PUFA	Total FA
24	Vehicle	322.09 ± 38.38	170.21 ± 41.37	103.94 ± 9.56	349.80 ± 42.12	946.04 ± 119.47
	TCDD	327.67 ± 14.47	197.54 ± 54.99	106.95 ± 10.60	363.20 ± 32.40	995.37 ± 99.90
	PCB153	304.38 ± 35.47	134.35 ± 31.72	103.70 ± 11.67	331.29 ± 26.02	873.73 ± 80.71
	MIX	350.49 ± 14.14	264.58 ± 27.06*a	114.20 ± 6.99	447.42 ± 29.96*ab	1176.69 ± 73.34*a
72	Vehicle	311.76 ± 32.18	184.24 ± 33.04	93.26 ± 10.15	317.51 ± 22.72	906.77 ± 60.97
	TCDD	353.26 ± 29.51	394.28 ± 63.50*a	109.14 ± 2.92	432.07 ± 40.07*	1288.74 ± 126.72*a
	PCB153	326.72 ± 45.42	213.53 ± 100.64	98.27 ± 15.94	326.28 ± 64.06	964.8 ± 191.49
	MIX	327.58 ± 22.21	257.33 ± 67.52	104.47 ± 5.89	394.45 ± 23.05	1083.84 ± 115.65
168	Vehicle	297.26 ± 6.39	178.44 ± 24.29	97.07 ± 7.28	333.55 ± 14.33	906.32 ± 33.60
	TCDD	384.92 ± 44.64*	432.65 ± 75.20*a	130.39 ± 6.76*a	526.26 ± 46.53*a	1474.21 ± 160.53*a
	PCB153	329.79 ± 46.76	184.20 ± 19.16	104.39 ± 8.46	342.23 ± 26.61	960.61 ± 95.75
	MIX	383.33 ± 14.70*	272.31 ± 62.84*ab	121.32 ± 11.21*a	461.61 ± 41.32*a	1238.56 ± 107.18*ab

Hepatic fatty acids were measured by GC-MS. Peak areas were integrated using MassLynx software. The results are displayed in arbitrary units and reported as mean ± SD of 5 independent replicates. Data were analyzed by ANOVA followed by Tukey's post hoc test: *$p<0.05$ vs. vehicle, a$p<0.05$ vs. PCB153 and b$p<0.05$ vs. TCDD.

FA – fatty acids; SFA – saturated fatty acids; MUFA – monounsaturated fatty acids; PUFA – polyunsaturated fatty acids. TCDD and PCB153 data are from Kopec et al. (2010b).

Toxicol Appl Pharmacol. Author manuscript; available in PMC 2014 August 08.

Table 2

Functional categorization and potential response element regulation of select hepatic genes differentially expressed by 30 μg/kg TCDD, 300 mg/kg PCB153, and MIX.

Functional category	Gene ID	Gene name	Gene symbol	TCDD*	PCB153*	MIX*	DREs[a]	PXREs[a]	CAREs[a]
Xenobiotic metabolism/ Oxidoreductase activity/ Oxidative stress	11761	Aldehyde oxidase 1	Aox1	2.2	2.9	4.8	yes	yes	yes
	11997	Aldo-keto reductase family 1, member B7	Akr1b7	NC	22.1	16.8	yes	yes	yes
	432720	Aldo-keto reductase family 1, member C19	Akr1c19	NC	1.7	2.0	yes	yes	no
	116852	Aldo-keto reductase family 1, member C20	Akr1c20	−1.7	−1.6	−3.0	no	yes	no
	13076	Cytochrome P450, family 1, subfamily a, polypeptide 1	Cyp1a1	348.1	NC	348.2	yes	yes	yes
	13077	Cytochrome P450, family 1, subfamily a, polypeptide 2	Cyp1a2	2.4	1.7	2.4	yes	yes	yes
	13088	Cytochrome P450, family 2, subfamily b, polypeptide 10	Cyp2b10	NC	16.1	24.2	yes	yes	yes
	13089	Cytochrome P450, family 2, subfamily b, polypeptide 13	Cyp2b13	NC	1.9	1.9	yes	yes	yes
	13094	Cytochrome P450, family 2, subfamily b, polypeptide 9	Cyp2b9	NC	7.6	6.2	no	yes	yes
	72082	Cytochrome P450, family 2, subfamily c, polypeptide 55	Cyp2c55	NC	48.4	48.4	yes	yes	yes
	13112	Cytochrome P450, family 3, subfamily a, polypeptide 11	Cyp3a11b	−1.9	4.0	3.1	yes	yes	yes
	13113	Cytochrome P450, family 3, subfamily a, polypeptide 13	Cyp3a13	−1.9	2.5	NC	no	yes	no
	56388	Cytochrome P450, family 3, subfamily a, polypeptide 25	Cyp3a25	NC	3.8	3.0	no	yes	yes
	56050	Cytochrome P450, family 39, subfamily a, polypeptide 1	Cyp39a1	NC	2.5	2.0	yes	yes	no
	14776	Glutathione peroxidase 2	Gpx2	NC	4.3	8.9	yes	yes	yes
	14858	Glutathione S-transferase, alpha 2 (Yc2)	Gsta2	5.8	4.1	11.3	yes	yes	yes
	14863	Glutathione S-transferase, mu 2	Gstm2	2.0	2.0	2.2	yes	yes	yes
	14865	Glutathione S-transferase, mu 4	Gstm4	2.4	4.0	5.6	yes	yes	yes
	14872	Glutathione S-transferase, theta 2	Gstt2	2.0	2.0	2.2	yes	yes	yes
	18104	NAD(P)H dehydrogenase, quinone 1	Nqo1s	4.6	2.8	12.6	yes	yes	yes
	76650	Sulfiredoxin 1 homolog (S. cerevisiae)	Srxn1s	2.6	2.3	3.9	yes	yes	yes
	394435	UDP glucuronosyltransferase 1 family, polypeptide A6B	Ugt1a6b	5.6	NC	6.4	yes	yes	no
	22235	UDP-glucose dehydrogenase	Ugdh	2.7	2.5	2.7	yes	yes	yes
	12491	CD36 antigen	Cd36	5.7	NC	6.1	yes	yes	yes
	26903	Dysferlin	Dysfs	3.3	1.5	14.9	yes	yes	yes
	170439	ELOVL family member 6, elongation of long chain fatty acids (yeast)	Elovl6	−4.3	−3.8	−5.2	yes	yes	yes
Lipid and glucose metabolism	75497	Fatty acid binding protein 12	Fabp12	53.7	−1.5	34.4	yes	yes	yes

Functional category	Gene ID	Gene name	Gene symbol	TCDD*	PCB153*	MIX*	DREs[a]	PXREs[a]	CAREs[a]
	14104	Fatty acid synthase	Fasn	−4.3	−3.9	−6.4	yes	yes	yes
	14718	Glutamate oxaloacetate transaminase 1, soluble	Got1	−2.6	NC	−4.3	yes	yes	yes
	14571	Glycerol phosphate dehydrogenase 2, mitochondrial	Gpd2	−3.0	1.5	−3.3	yes	yes	yes
	72999	Insulin induced gene 2	Insig2	NC	5.9	4.0	yes	yes	yes
	53357	Phospholipase A2, group VI	Pla2g6	NC	2.5	1.8	yes	yes	yes
	66350	Phospholipase A2, group XIIA	Pla2g12as	3.7	2.7	7.7	yes	yes	yes
	228026	Pyruvate dehydrogenase kinase, isoenzyme 1	Pdk1	−1.6	NC	1.6	yes	yes	no
	20250	Stearoyl-Coenzyme A desaturase 2	Scd2	2.0	NC	NC	yes	yes	yes
	20788	Sterol regulatory element binding factor 2	Srebf2	−1.7	−2.1	−1.6	yes	yes	yes
	20787	Sterol regulatory element binding transcription factor 1	Srebf1	−2.3	−2.4	−4.6	yes	yes	yes
Cell cycle/Cell death	12125	BCL2-like 11 (apoptosis facilitator)	Bcl2l11	1.9	NC	4.2	yes	yes	no
	13197	Growth arrest and DNA-damage-inducible 45 alpha	Gadd45a	−3.6	9.4	3.1	yes	no	yes
	17873	Growth arrest and DNA-damage-inducible 45 beta	Gadd45b	5.7	10.8	29.2	yes	yes	yes
	53415	HIV-1 tat interactive protein 2, homolog (human)	Htatip2	3.5	NC	4.4	yes	yes	no
	15937	Immediate early response 3	Ier3	3.5	NC	3.8	yes	yes	yes
	17869	Myelocytomatosis oncogene	Myc	3.0	4.2	7.2	yes	yes	yes
	211323	Neuregulin 1	Nrg1	2.8	NC	6.7	yes	yes	yes
	78688	Nucleolar protein 3 (apoptosis repressor with CARD domain)	Nol3	NC	4.8	4.7	yes	yes	no
	22033	Tnf receptor-associated factor 5	Traf5	2.1	NC	2.3	yes	yes	yes
	21813	Transforming growth factor, beta receptor II	Tgfbr2	1.6	1.8	2.4	yes	yes	yes
	29820	Tumor necrosis factor receptor superfamily, member 19	Tnfrsf19	3.9	2.6	7.7	yes	yes	yes
	21928	Tumor necrosis factor, alpha-induced protein 2	Tnfaip2	6.7	NC	6.9	yes	yes	yes
	66443	Tumor necrosis factor, alpha-induced protein 8-like 1	Tnfaip8l1	3.0	NC	4.1	yes	yes	yes
Immune response	12774	Chemokine (C-C motif) receptor 5	Ccr5	2.4	−1.6	NC	no	yes	yes
	56644	C-type lectin domain family 7, member a	Clec7a	3.9	NC	2.9	yes	yes	yes
	58239	Dexamethasone-induced transcript	Dexi	−1.9	−1.9	−4.3	yes	yes	no
	14129	Fc receptor, IgG, high affinity I	Fcgr1	2.4	NC	1.9	yes	yes	no
	14969	Histocompatibility 2, class II antigen E beta	H2-Eb1	7.8	NC	5.0	yes	yes	yes
	14998	Histocompatibility 2, class II, locus DMa	H2-DMa	4.0	NC	2.7	yes	yes	yes
	14999	Histocompatibility 2, class II, locus Mb1	H2-DMb1	4.9	NC	3.2	yes	yes	yes
	15900	Interferon regulatory factor 8	Irf8	3.1	NC	2.0	yes	yes	yes

Functional category	Gene ID	Gene name	Gene symbol	TCDD*	PCB153*	MIX*	DREs[a]	PXREs[a]	CAREs[a]
	16994	Lymphotoxin B	Ltb	2.9	NC	2.3	yes	yes	yes
	17304	Milk fat globule-EGF factor 8 protein	Mfge8	4.6	NC	5.0	yes	yes	yes
	20719	Serine (or cysteine) peptidase inhibitor, clade B, member 6a	Serpinb6as	5.1	NC	11.0	yes	yes	yes
	20208	Serum amyloid A 1	Saa1	3.4	NC	3.2	yes	yes	no
	20209	Serum amyloid A 2	Saa2	3.2	NC	3.2	yes	yes	yes
	20210	Serum amyloid A 3	Saa3	7.8	NC	3.5	yes	yes	no

NC - no change.

*Maximum fold change on the microarray (|fold change| >1.5, P1(t) > 0.90).

[a]Putative DNA response elements identified by computational searches (see *Materials and Methods*).

[b]QRTPCR results. The Agilent microarray Cyp3a11 probe maps the 60-mer region between positions 1105 and 1164 of the Cyp3a11 gene, which is 2053 bp long, while Cyp3a11 primers (listed in a Supplementary Table 3) amplify the 119 bp fragment between 1701 and 1819 bp suggesting that both approaches amplify non-overlapping regions of the gene.

[s]Synergistic response verified by non-linear logistic modeling of QRTPCR dose-response data.